



This is to certify that the thesis entitled

TEMPERATURE DEPENDENCE, STRUCTURAL PLASTISCITY, AND RESONANCE ASSIGNMENT OF UNIFORMLY LABELED HIV-1 FUSION PEPTIDES ASSOCIATED WITH MEMBRANES

presented by

Michele L. Bodner

has been accepted towards fulfillment of the requirements for the

M. S.	degree in	Chemistry
	David P.	Weliky fessor's Signature
	Major Pro	fessor's Signature
	Dec.	10, 2003
		Date

MSU is an Affirmative Action/Equal Opportunity Institution

LIBRARY Michigan State University

PLACE IN RETURN BOX to remove this checkout from your record.

TO AVOID FINES return on or before date due.

MAY BE RECALLED with earlier due date if requested.

DATE DUE	DATE DUE	DATE DUE

6/01 c:/CIRC/DateDue.p65-p.15

TEMPERATURE DEPENDENCE, STRUCTURAL PLASTICITY, AND RESONANCE ASSIGNMENT OF UNIFORMLY LABELED HIV-1 FUSION PEPTIDES ASSOCIATED WITH MEMBRANES

Ву

Michele L. Bodner

A THESIS

Submitted to
Michigan State University
in partial fulfillment of the requirements
for the degree of

MASTER OF SCIENCE

Department Of Chemistry

ABSTRACT

TEMPERATURE DEPENDENCE, STRUCTURAL PLASTICITY, AND RESONANCE ASSIGNMENT OF UNIFORMLY LABELED HIV-1 FUSION PEPTIDES ASSOCIATED WITH MEMBRANES

By

Michele L. Bodner

The HIV-1 viral fusion peptide serves as a biologically relevant model for viral/target cell membrane fusion and in my work, the structure of the membraneassociated peptide was probed by solid state NMR MAS ¹³C chemical shift measurements. Solution NMR studies have shown that the peptide is predominantly helical in detergent micelles and this was correlated with solid state NMR ¹³C chemical shifts in frozen detergent. Large shift changes (2-4 ppm) were observed for the peptide in a mixture whose lipid headgroup and cholesterol composition reflects the membranes of host cells of the virus. In this more biologically relevant composition, the chemical shifts are consistent with predominant non-helical structure. NMR spectra were compared at -50 °C and at 20 °C. Similar peak chemical shifts were observed at both temperatures, which indicates that cooling the sample does not significantly change the peptide structure. Relative to -50 °C, the 20 °C signals were narrower and had lower intensity, which is consistent with greater motion at higher temperature. ¹³C/¹³C correlation experiments were performed on a sample in which the peptide was U-13C/15N labeled over three or twelve sequential residues. The resulting 2D spectra were used to assign the ¹³C chemical shifts in the labeled residues and the shifts were consistent with beta strand structure. ¹⁵N-¹³C correlation experiments were also done on a uniformly ¹³C/¹⁵N N-Acetyl-leucine model compound sample.

To Mom and Dale

Acknowledgements

I would like to thank my advisor, Dr. David Weliky, and the Weliky group for their help and support during the last couple of years. I also want to thank my family and friends for all their support.

•

TABLE OF CONTENTS

LISTOFT	ABLES	Page
LIST OF TA	ADLES	V
LIST OF FI	GURES	vi
LIST OF AI	BBREVIATIONS	x
Chapter 1	Introduction	1
•	References	7
Chapter 2	Experimental: 1D REDOR Filtering and 2D ¹³ C- ¹³ C Correlation	
	Materials	
	Peptides	
	Lipid Preparation	
	Cross-Linking	
	Solid State NMR Sample Preparation	
	Magic Angle Spinning	13
	¹³ C CP MAS Experiments	13
	Filtering Methods	15
	NMR Spectroscopy-Experimental Details	
	1D REDOR Experimental Details	17
	2D Experimental Details	18
	References	23
Chapter 3	Results and Discussion: 1D REDOR Filtering and 2D ¹³ C- ¹³ C	
	Correlation	
	Utility of REDOR Filtering	25
	Comparison of HFP Spectra in Detergent and Membranes	27
	Temperature Dependence of Spectra	29
	2D Correlation Spectra	29
	References	43
Chapter 4	¹⁵ N- ¹³ C Correlation Experiments	45
	Introduction	
	N-Acetyl-leucine Synthesis and Crystallization	45
	1D ¹⁵ N- ¹³ C Correlation Experiments	46
	Results and Discussion	46
	Conclusions	50
	References	
Chapter 5	Conclusions and Future Work	52
-	Temperature Dependence of Spectra	52
	2D ¹³ C- ¹³ C and ¹⁵ N- ¹³ C Correlation	
	References	

LIST OF TABLES

	1	Pages
Table1.	¹³ C chemical shift assignment for LM3-associated HFP-U3	34
Table2.	¹³ C chemical shift assignment for LM3-associated HFP-U12 dimer	42

LIST OF FIGURES

Pages
Figure 1. Model (left) and Electron Microscopy (right) of the HIV virus (a) binding to host cell (b) fusion of viral and host cell membranes (c,d) formation of large pore and infection of host cell. The Triangle represents the viral RNA that enters the host cell 2
Figure 2. Model of HIV Infection. FP= Fusion Peptide. Time Sequence: Left to Right.
Figure 3. Model for HIV-1/Host cell fusion. In the left-most figure, a gp120/gp40 trimer is displayed with the balls representing gp120 and rods representing gp41. F represents the fusion peptide and A represents the transmembrane anchorage of gp41. Fusion proceeds temporally from left to right with (i) initial state, (ii) receptor binding and fusion peptide membrane insertion, (iii) gp41 conformational change, and (iv) membrane fusion
Figure 4. Chemical structure of HFP-U3 showing ¹³ C and ¹⁵ N labeling
Figure 5. ¹³ C CP MAS sequence. Magnetization was transferred from protons to ¹³ C during CP. ¹ H continuous wave decoupling was applied during acquisition
Figure 6. 1D ¹³ C REDOR pulse sequence. CP transferred proton magnetization to ¹³ C. ¹³ C magnetization is dephased (reduced) by ¹³ C- ¹⁵ N dipolar coupling mediated by two equally spaced ¹⁵ N 180° pulses per rotor period. A ¹³ C 180° pulse in the middle of the dephasing period refocuses the ¹³ C chemical shift
Figure 7. 2D 13 C correlation PDSD sequence. Magnetization was transferred from 1 H to 13 C during CP. Continuous wave (CW) decoupling is applied after CP on the protons during t_1 and t_2 , but not during τ . t_1 was the evolution time, τ was the magnetization exchange time, and t_2 was the acquisition time
Figure 8. 2D ¹³ C- ¹³ C correlation RFDR sequence. CP transferred magnetization from ¹ H to ¹³ C and evolves during t ₁ . The τ exchange period consists of ¹³ C 180° pulses every other rotor period. Acquisition was done during t ₂
Figure 9. 13 C solid-state NMR spectra of HFP-U3 peptide associated with LM3 lipid mixture at -50° C. (top) Unfiltered REDOR spectrum where signal from both the lipids and peptide are observed. (bottom) Filtered spectrum obtained from the difference of S_0 - S_1 FIDs. Because of the short 1.6 ms dephasing time only the backbone carbonyl and C_{α} signals from Phe-8, Leu-9, and Gly-10 are observed. * = Carbonyl spinning sidebands.

Figure 10. ¹³ C solid state NMR spectra of HFP-U3 associated with DPC at -80°C (top) and LM3 lipid mixture at -50°C (bottom). The peptide had uniform ¹³ C, ¹⁵ N labeling at the Phe-8, Leu-9, and Gly-10 residues. Because of the 1ms REDOR filter, the spectra are dominated by backbone carbonyl signals from Phe-8 and Leu-9 and backbone C _α signals from Phe-8, Leu-9, and Gly-10. For each spectrum, the spinning speed was 8 kHz and 50 Hz gaussian line broadening was applied. The large differences between chemical shifts in (top) and (bottom) spectra are consistent with a change from helical structure in detergent to non-helical structure in LM3
Figure 11. ¹³ C solid state NMR spectra of HFP-U3 associated with LM3 lipid mixture at -50 °C (top) and 20 °C. The chemical shifts in the spectra are consistent with non-helical structure at both -50 °C and 20 °C. However, the -50 °C spectrum has about three times more integrated signal per scan than the 20 °C spectrum, which can be explained by greater motion at 20 °C.
Figure 12. (a) 2D 13 C- 13 C contour plot spectrum of HFP-U3 associated with LM3 lipid mixture at -50 °C and (b) f_2 slices from this spectrum. The peptide: lipid mol ratio was \sim 0.04, the buffer pH was 7.0, and the sample volume in the 4mm diameter rotor was \sim 30 µl. The peptide had uniform 13 C, 15 N labeling at the Phe-8, Leu-9, and Gly-10 residues. The 2D data were obtained with a proton-driven spin diffusion sequence and the total signal averaging time was \sim 54 hours. The spectrum displayed in (a) was processed with 200 Hz Gaussian line broadening in f_1 and 150 Hz line broadening in f_2 . Ten contours are shown with each increasing contour representing 1.5 times greater signal intensity. In the upper slice of (b), cross peaks to the Phe-8 aromatic C1 (f_1 = 137.6 ppm) are displayed. From left to right, they represent magnetization in f_2 on the following Phe-8 nuclei: CO, aromatic C1(diagonal), aromatic C2-C6, C_{α} , and C_{β} . In the lower slice of (b), cross peaks to the Leu-9 CO (f_1 = 172.1ppm) are displayed. From left to right, they represent magnetization in f_2 on the following Leu-9 nuclei: CO (diagonal), CO (m =-1 spinning sideband), C_{α} , C_{β} , C_{γ} with C_{δ} shoulder, and CO (m = -2 spinning sideband)
Figure 13. 2D ¹³ C- ¹³ C contour plot spectrum of HFP-U3 associated with LM3 lipid mixture. The 2D data set was obtained with a radio frequency- driven recoupling sequence using a 4 ms RFDR mixing time
Figure 14. Secondary ¹³ C chemical shifts for Phe-8, Leu-9, and Gly-10 of HFP-U3 associated with LM3 lipid mixture. Vertical bars represent the secondary shifts for each residue. For these three residues, the pattern shown above is indicative of a β strand structure
Figure 15. 2D ¹³ C- ¹³ C contour plot spectrum of HFP-U3 associated with LM3 lipid mixture at -50 °C. The 2D data was obtained with a proton-driven spin diffusion sequence using a 100ms exchange time. The cross peak between Phe ar. 2-6 and Leu C _γ is observed because of the longer exchange time. 37
Figure 16. 13 C solid state NMR spectrum of HFP–U12 dimer associated with LM3 at –50°C. Due to a 1 ms REDOR filter time only the backbone carbonyl and C_{α} signals are

observed. Other experimental conditions were: 4 mm rotor diameter; 8 kHz MAS frequency; and 50 Hz line broadening
Figure 17. 2D ¹³ C- ¹³ C contour plot spectrum of HFP–U12 dimer associated with LM3 lipid mixture. The 2D data was obtained using a proton-driven spin diffusion sequence with a 10 ms exchange time
Figure 18. 2D ¹³ C- ¹³ C contour plot spectrum of HFP-U12 dimer associated with LM3 lipid mixture. The 2D data was obtained using a radio frequency-driven recoupling sequence with a 4 ms RFDR mixing time
Figure 19. Chemical structure of U-N-Acetyl-leucine showing ¹³ C and ¹⁵ N labeling 47
Figure 20. 1D ¹⁵ N- ¹³ C correlation sequence. CP1 transfers magnetization from protons to ¹⁵ N. CP2 transfers magnetization from ¹⁵ N to ¹³ C followed by ¹³ C detection
Figure 21. Crystalline N-Acetyl-Leucine model compound uniformly ¹³ C/ ¹⁵ N labeled. The spectra were obtained at –50 °C, MAS frequency of 6.8 kHz, and 32 scans of signal averaging. (bottom) ¹³ C CP MAS all labeled carbons were observed. (middle) 1D ¹ H- ¹⁵ N- ¹³ C selective CP spectrum dominant signal from the carbonyl directly bonded to ¹⁵ N. (Top) 1D ¹ H- ¹⁵ N- ¹³ C selective CP spectrum dominant signal from the C _α
Figure 22. 2D ¹⁵ N- ¹³ C correlation sequence. CP1 transferred magnetization from protons to ¹⁵ N, which then evolved during t ₁ . CP2 transferred magnetization from ¹⁵ N to ¹³ C and was detected during t ₂

LIST OF ABBREVIATIONS

AIDS Acquired Immune Deficiency Syndrome

CP Cross Polarization

CW Continuous Wave

DPC Dodecylphosphocholine

FMOC 9-Fluorenylmethoxycarbonyl

FWHM Full-Width-at-Half-Maximum

HEPES N-2-Hydroxyethylpiperazine-N'-2-Ethanesulfonic acid

HIV Human Immunodeficiency Virus

HPLC High Performance Liquid Chromatography

LUV Large Unilamellar Vesicles

MALDI Matrix Assisted Laser Desorption Ionization

MAS Magic Angle Spinning

NMR Nuclear Magnetic Resonance

PDSD Proton Driven Spin Diffusion

PI Phosphatidylinositol

POPC 1-Palmitoyl-2-Oleoyl-sn-glycero-3-Phosphocholine

POPE 1-Palmitoyl-2-Oleoyl-sn-glycero-3-Phosphoethanolamine

POPS 1-Palmitoyl-2-Oleoyl-sn-glycero-3-[Phospho-L-Serine]

ppm parts per million

REDOR Rotational Echo Double Resonance

RF Radio Frequency

RFDR Radio Frequency Driven Recoupling

SSNMR Solid State Nuclear Magnetic Resonance

TFA Trifluoroacetic Acid

TPPM Two Pulse Phase Modulation

Chapter 1

Introduction

Fusion between cells and cellular components plays an important role in such significant physiological processes as egg fertilization and synaptic transmission in the nervous system. Membrane fusion is also an important step in viral infection for such widespread and serious diseases as measles, influenza and AIDS.¹⁻³ Understanding viral fusion is important as a key step in the viral life cycle and as a possible target for antiviral therapeutics.

Many viruses are "enveloped", i.e. they are enclosed by a membrane. To initiate infection of a new cell, the membranes of the virus and cell must fuse so that the viral nucleic acid can enter the host cell. ^{1, 2, 4, 5} Figure 1⁶ illustrates the three sequential steps of fusion: binding of the two membranes, mixing of lipid membranes, and formation of a large pore through which the contents of both the virus and the host cell mix. ⁷ There is a high activation barrier to membrane fusion and in the absence of a catalyst, the viral fusion rate is usually negligible. Fusion is also very slow between unilamellar liposomes, which often serve as a model membrane system for viruses or cells. To increase the fusion rate, many viruses such as HIV-1 employ a "fusion peptide" which represents a ~20-residue apolar domain at the N-terminus of the viral envelope fusion protein. ^{3, 8}

Current models of HIV-1/host cell infection include interaction of the fusion peptide with the host cell membrane as displayed in figures 2° and 3¹⁰. Fusion and infection are initiated by strong interactions of two viral enveloped proteins (gp41 and

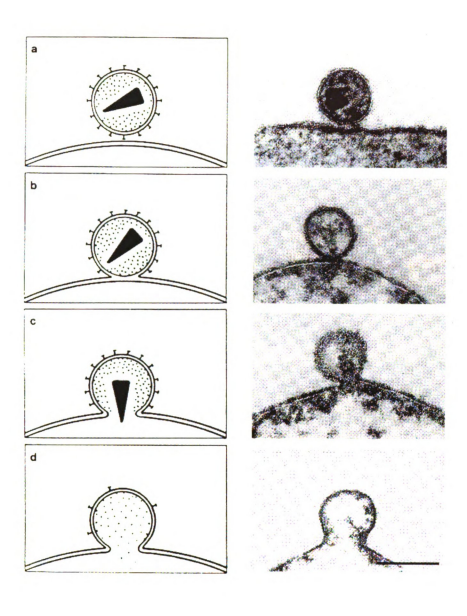


Figure 1. Model (left) and Electron Microscopy (right) of the HIV virus (a) binding to host cell (b) fusion of viral and host cell membranes (c,d) formation of large pore and infection of host cell. The triangle represents the viral RNA that enters the host cell.

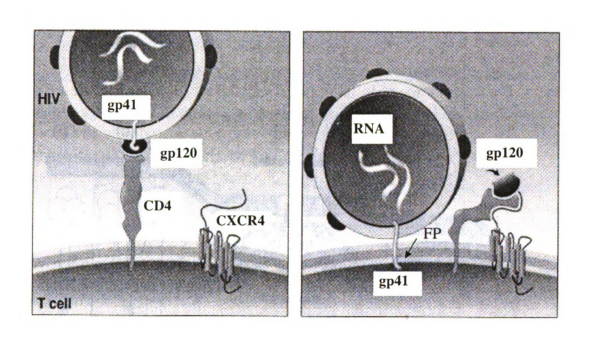


Figure 2. Model of HIV Infection. FP= Fusion Peptide. Time Sequence: Left to Right

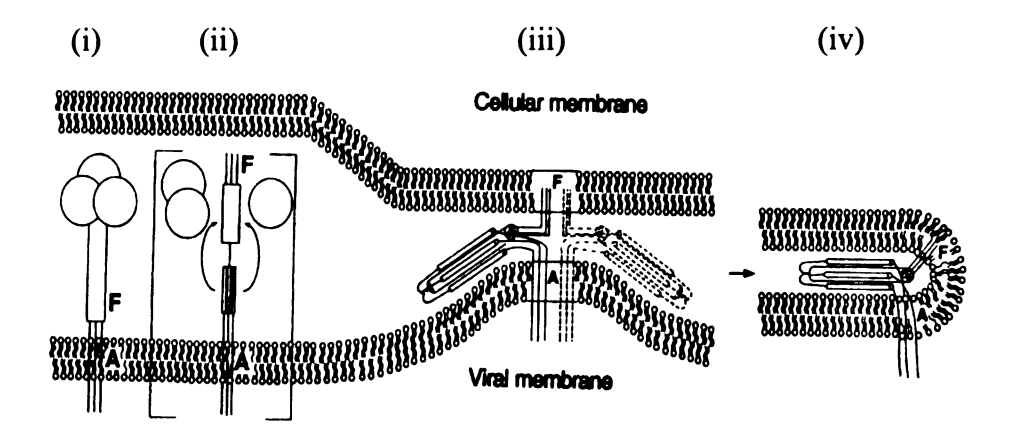


Figure 3. Model for HIV-1/Host cell fusion. In the left-most figure, a gp120/gp40 trimer is displayed with the balls representing gp120 and rods representing gp41. F represents the fusion peptide and A represents the transmembrane anchorage of gp41. Fusion proceeds temporally from left to right with (i) initial state, (ii) receptor binding and fusion peptide membrane insertion, (iii) gp41 conformational change, and (iv) membrane fusion.

gp120) with the CD4 and chemokine (e.g. CXCR4) receptors of human T and macrophage cells. 11, 12 gp41 traverses the HIV-1 membrane and the fusion peptide region is located at the N-terminus of the gp41 extraviral ectodomain.

Because of the hydrophobic nature of this region and the presence of the lipid membrane, the fusion peptide region has not been studied in membranes with atomic-level structural techniques, such as crystallography or solution nuclear magnetic resonance. Solid state NMR, however, can be applied to obtain atomic-resolution structural information about the fusion peptide in a fully hydrated lipid membrane environment, and the structural information can be related to function.

Solid state NMR of peptides and proteins has traditionally relied on selective ¹³C and ¹⁵N labeling and by this approach the determination of a complete structure requires at least one selectively labeled sample per residue. Preparation of such a large number of samples is time consuming and complete structures of only two membrane-bound peptides have been reported with this methodology. ^{13, 14} Recently, there has been an effort to develop an alternate solid state NMR approach in which a complete structure is derived from a single uniformly ¹³C/¹⁵N labeled sample. This methodology requires multidimensional NMR techniques for uniquely assigning the chemical shifts of each ¹³C and ¹⁵N nucleus and multidimensional NMR techniques to determine internuclear distance and angle constraints. ¹⁵⁻²⁰ A whole protein structure would then be developed through molecular dynamic simulations, which incorporate the constraints. The overall approach is analogous to the well-developed NMR methods for proteins and nucleic acids in aqueous solution and has the potential to provide high-resolution structures for small proteins in intact biological membranes. The solid state NMR (SSNMR) approach will

be complementary to solution NMR and crystallographic methods for membrane proteins, which are typically done in detergent environments. This thesis describes application of this type of SSNMR approach to the membrane-associated HIV-1 fusion peptide.

References

- 1. Blumenthal, R. and D.S. Dimitrov, *Membrane Fusion*, in *Handbook of Physiology*, *Section 14: Cell Physiology*, J.F. Hoffman and J.C. Jamieson, Editors. 1997, Oxford: New York. p. 563-603.
- 2. Dimitrov, D.S., Cell biology of virus entry. Cell, 2000. 101(7): p. 697-702.
- 3. Eckert, D.M. and P.S. Kim, *Mechanisms of viral membrane fusion and its inhibition*. Annual Review of Biochemistry, 2001. **70**: p. 777-810.
- 4. Blumenthal, R., et al., *Membrane fusion*. Chemical Reviews, 2003. **103**(1): p. 53-69.
- 5. Epand, R.M., *Membrane fusion Overview*. Bioscience Reports, 2000. **20**(6): p. 435-441.
- 6. Grewe, C., Beck, A., Gelderblom, H.R., *HIV: early virus-cell interactions*. Journal of Acquired Immune Dificiency Syndromes, 1990. **3:** p. 965.
- 7. Hernandez, L.D., et al., *Virus-cell and cell-cell fusion*. Annual Review of Cell Developmental Biology, 1996. **12**: p. 627-61.
- 8. Durell, S.R., et al., What studies of fusion peptides tell us about viral envelope glycoprotein-mediated membrane fusion (review). Molecular Membrane Biology, 1997. 14(3): p. 97-112.
- 9. Breakthrough of the Year: New Hope in HIV Disease. Science, New Series. 274: p. 1988-1991.
- 10. Weissenhorn, W., Dessen, A., Harrison, S.C., Skehel, J.J., Wiley, D.C., Atomic Structure of the Ectodomain from HIV-1 gp41. Nature. 387: p. 426.
- 11. Bleul, C.C., Farzan, M., Choe, H., Parolin, C., ClarkLewis, I., Sodroski, J., Springer, T.A, The lymphocyte chemoattractant SDF-1 is a ligand for LESTR/fusin and blocks HIV-1 entry. Nature, 1996. 382: p. 829-833.
- 12. Oberlin, E., Amara, A., Bachelerie, F., Bessia, C., Virelizier, J. L., ArenzanaSeisdedos, F., Schwartz, O., Heard, J.M., ClarkLewis, I., Legler, D.F., Loetscher, M., Baggiolini, M., Moser, B., The CXC chemokine SDF-1 is the ligand for LESTR/. Fusin and prevents infection by T-cell-line adapted HIV-1. Nature, 1996. 382: p. 833-835.

- 13. Ketchem, R.R., W. Hu, and T.A. Cross, *High-resolution conformation of gramicidin A in a lipid bilayer by solid-state NMR*. Science, 1993. **261**(5127): p. 1457-60.
- 14. Opella, S.J., et al., Structures of the M2 channel-lining segments from nicotinic acetylcholine and NMDA receptors by NMR spectroscopy. Nature Structural Biology, 1999. 6(4): p. 374-9.
- 15. Rienstra, C.M., et al., 2D and 3D N-15-C-13-C-13 NMR chemical shift correlation spectroscopy of solids: Assignment of MAS spectra of peptides. Journal of the American Chemical Society, 2000. 122(44): p. 10979-10990.
- 16. McDermott, A., et al., Partial NMR assignments for uniformly (C-13, N-15)-enriched BPTI in the solid state. Journal of Biomolecular NMR, 2000. 16(3): p. 209-219.
- 17. Pauli, J., et al., Backbone and side-chain C-13 and N-15 signal assignments of the alpha-spectrin SH3 domain by magic angle spinning solid-state NMR at 17.6 tesla. Chembiochem, 2001. 2(4): p. 272-281.
- 18. Egorova-Zachernyuk, T.A., et al., Heteronuclear 2D-correlations in a uniformly [C-13, N-15] labeled membrane-protein complex at ultra-high magnetic fields. Journal of Biomolecular NMR, 2001. 19(3): p. 243-253.
- 19. Castellani, F., et al., Structure of a protein determined by solid-state magic-angle-spinning NMR spectroscopy. Nature, 2002. **420**(6911): p. 98-102.
- 20. Detken, A., et al., Methods for sequential resonance assignment in solid, uniformly C-13, N-15 labelled peptides: Quantification and application to antamanide. Journal of Biomolecular NMR, 2001. 20(3): p. 203-221.

Chapter 2

Experimental: 1D REDOR Filtering and 2D ¹³C-¹³C Correlation

Materials

Rink amide resin was purchased from Advanced Chemtech (Louisville, KY), and 9-fluorenylmethoxycarbonyl (FMOC)-amino acids were obtained from Peptides
International (Louisville, KY). Isotopically labeled amino acids were purchased from Cambridge (Andover, MA) and were FMOC-protected using literature procedures. 1-2 1-palmitoyl-2-oleoyl-sn-glycero-3-phosphocholine (POPC), 1-palmitoyl-2-oleoyl-sn-glycero-3-[phospho-L-serine] (POPS), 1-palmitoyl-2-oleoyl-sn-glycero-3-phosphoethanolamine (POPE), phosphatidylinositol (PI), sphingomyelin, and dodecylphosphocholine (DPC) were purchased from Avanti Polar Lipids, Inc. (Alabaster, AL). N-2-hydroxyethylpiperazine-N'-2-ethanesulfonic acid (HEPES) was obtained from Sigma (St. Louis, MO). All other reagents were analytical grade.

Peptides

HFP-U3 fusion peptide (sequence AVGIGALFLGFLGAAGSTMGARSKKK)

(figure 4) was synthesized with the 23 N-terminal residues of the LAV_{1a} strain of the HIV-1 gp41 envelope protein followed by three additional lysines for improved solubility. HFP-U12 fusion peptide (sequence AVGIGALFLGFLGAAGSTMGARSCKKKKKW) was synthesized with the 23 N-terminal residues of the LAV_{1a} strain of the HIV-1 gp41 envelope protein followed by a cysteine to allow for cross-linking of the peptide. The whole gp41 protein is believed to

Figure 4. Chemical structure of HFP-U3 showing ¹³C and ¹⁵N labeling.

be trimeric with the C-termini of three fusion peptides in close proximity (Figure 3), so the topology gained through peptide cross-linking is likely similar to the topology which exists in the fusogenic form of gp41.³ As in HFP-U3, the six additional lysines are to enhance solubility. A single tryptophan was added as a 280 nm chromophore for peptide quantitation. Both peptides were synthesized as their C-terminal amides using a peptide synthesizer (ABI 431A, Foster City, CA) equipped with FMOC chemistry. HFP-U3 had uniform ¹³C and ¹⁵N labeling at Phe-8, Leu-9, and Gly-10 and HFP-U12 had uniform ¹³C and ¹⁵N labeling over the twelve residues between Gly-5 and Gly-16. Peptides were cleaved from the resin in a three hour reaction using a mixture of trifluoroacetic acid (TFA):H₂O:phenol:thioanisole:ethanedithiol in a 33:2:2:2:1 volume ratio. Peptides were subsequently purified by reversed-phased HPLC using a preparative C₁₈ column (Vydac, Hesperia, CA) and a water/acetonitrile gradient containing 0.1% TFA. Matrix assisted laser desorption ionization (MALDI) mass spectroscopy was used to determine the peptide products.

Lipid Preparation

Samples were prepared using a lipid/cholesterol mixture reflecting the approximate lipid and cholesterol content of the HIV-1 virus infected host cells.⁴ This lipid mixture consists of POPC, POPE, POPS, PI, sphingomyelin, and cholesterol in a 10:5:2:1:2:10 molar ratio. Lipid and cholesterol powders were dissolved together in chloroform. The chloroform was removed under a stream of nitrogen followed by overnight vacuum pumping. Lipid dispersions were formed by addition of buffer containing 0.01% NaN₃ followed by homogenization with ten freeze-thaw cycles. Large Unilamellar Vesicles (LUV) of 100 nm diameter were prepared by extruding the lipid

dispersions ~30 times through two stacked 0.1 μm polycarbonate filters⁵ (Avestin, Inc., Ottawa, ON, Canada).

Cross-Linking

The additional cysteine in HFP-U12 allows covalent cross-linking of two peptides through a disulfide bond. Peptide was dissolved into a 0.5 M dimethylaminopyridine buffer at pH 8.40. This solution was vortexed for 24 hours open to the air. Purification of the peptide dimer was carried out as described above for the monomeric peptides.

Solid State NMR Sample Preparation

Samples were prepared using 0.01% (w/v) NaN₃ in 5 mM HEPES buffer (pH 7.0). A solution was made containing 0.4 – 2 µmol peptide in 30 ml volume and a solution was made containing 100 nm diameter LUV in 5 ml volume. The LUV were made with 40 µmol lipid and 20 µmol cholesterol. The peptide and LUV solutions were then mixed and kept at room temperature overnight. The solution was then centrifuged at 100,000 – 130,000 * g for four hours to pellet down the LUV and associated bound peptide. Nearly all peptide bound to LUV under these conditions and unbound peptide does not pellet. The peptide/LUV pellet formed after ultracentrifugation was transferred by spatula to a 4 mm magic angle spinning (MAS) NMR rotor.

Peptide/detergent samples were prepared with 1.7-2 mM peptide in 200 mM DPC detergent with a total volume of 250 μ l. There was no ultracentrifugation step and the liquid was transferred by pipet to the 6 mm MAS NMR rotor.

For both the membrane and detergent samples, the MAS rotors were fitted with specially machined vespel caps. At liquid nitrogen temperatures, a cap inserted tightly

into the rotor. After the cap warmed up, it formed a very tight seal, which minimized dehydration of the samples.

Magic Angle Spinning (MAS)

In solids, there is negligible molecular tumbling and the NMR signals are broadened by anisotropic effects. These effects can be reduced and the lines narrowed by magic angle spinning (MAS), whereby the sample is rotated at kHz frequencies about an axis tilted at 54.7° relative to the external magnetic field direction. The MAS spectrum contains signals at the isotropic chemical shifts, i.e. the shifts which would be observed in a typical liquid state spectrum. If the spinning frequency is slow enough, additional signals are observed which are separated from the isotropic peaks by integral multiples of the spinning frequency and are known as spinning sidebands.

¹³C CP MAS Experiments

Transfer or "Cross polarization" (CP) of magnetization from protons to ¹³C is a SSNMR technique which increases ¹³C signals in 1D as well as multidimensional NMR experiments. CP is accomplished by simultaneous RF radiation of both the ¹H and ¹³C nuclei such that both isotopes precess at the same frequency. Magnetization transfer is mediated by heteronuclear dipolar coupling. Figure 5 shows the typical pulse sequence for a 1D ¹³C CP experiment including acquisition.

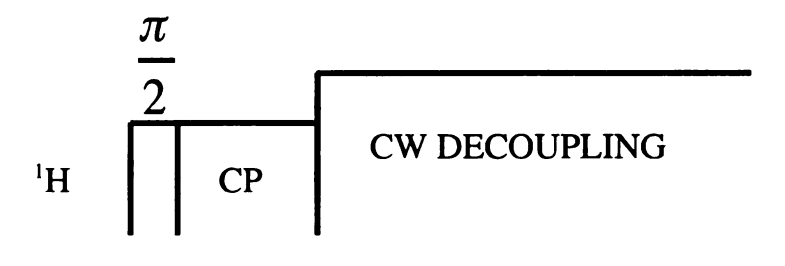




Figure 5. ¹³C CP MAS sequence. Magnetization was transferred from protons to ¹³C during CP. ¹H continuous wave decoupling was applied during acquisition.

Filtering Methods

In peptide/membrane samples containing specifically 13 C labeled peptide, 1 H- 13 C cross-polarized (CP) 13 C NMR spectra typically have very large lipid, cholesterol, and peptide natural abundance signals. Two approaches were taken to filter out the natural abundance signals. For 1D spectra, a rotational-echo double- resonance (REDOR) NMR filtering sequence was applied and the resulting spectra were dominated by labeled backbone 13 C with directly bonded 15 N. $^{6.7}$ For example, for the HFP-U3 sample, a clean spectrum was observed of the Phe-8, Leu-9, and Gly-10 C_{α} and the Phe-8 and Leu-9 CO carbons. In the second filtering approach, 2D 13 C- 13 C correlation spectra were obtained on both the HFP-U3 and HFP-U12 sample and off-diagonal cross peaks were only detected between labeled 13 C which are separated by one or a few bonds; i.e. in a strong 13 C- 13 C dipole coupling network.

The REDOR technique relies on the difference of two spectra, one with the REDOR sequence (Figure 6), and one with a REDOR sequence without ^{15}N π pulses. With ^{15}N pulses (S_1 spectrum), there is heteronuclear ^{13}C - ^{15}N dipolar coupling and the signals of ^{13}C directly bonded to ^{15}N are reduced. Without ^{15}N pulses (S_0 spectrum), there is no ^{13}C - ^{15}N dipolar coupling and the signals of all ^{13}C nuclei are equally detected. Thus, the $S_0 - S_1$ difference spectrum yields only the signals of ^{13}C directly bonded to ^{15}N .

NMR Spectroscopy – Experimental Details

The NMR spectra were taken on 9.4 T spectrometers (Varian Infinity Plus, Palo Alto, CA) using triple resonance MAS probes equipped for either 4 mm or 6 mm diameter rotors. The temperature was monitored by a thermocouple located about 1" from the rotor and in the flow of the cooling nitrogen gas. The actual temperature of the

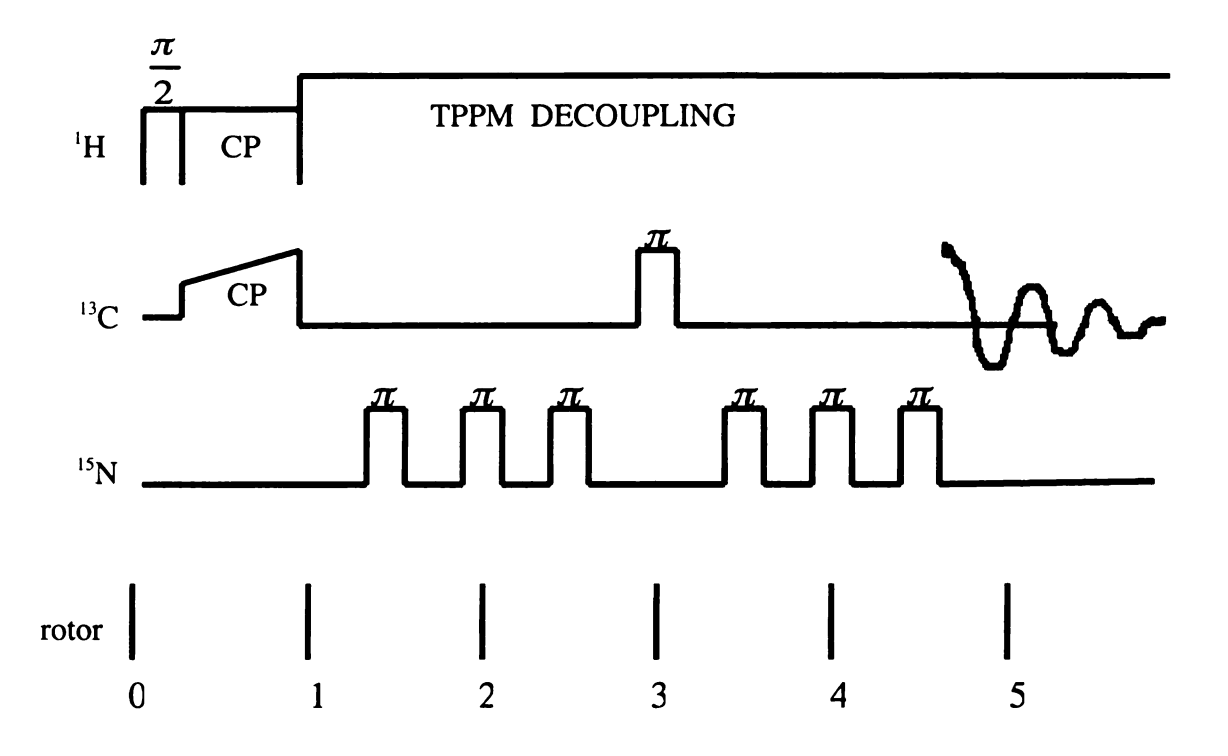


Figure 6. 1D ¹³C REDOR pulse sequence. CP transferred proton magnetization to ¹³C. ¹³C magnetization is dephased (reduced) by ¹³C-¹⁵N dipolar coupling mediated by two equally spaced ¹⁵N 180° pulses per rotor period. A ¹³C 180° pulse in the middle of the dephasing period refocuses the ¹³C chemical shift.

sample is likely warmer than the measured temperature because of frictional heating from sample spinning and from heating due to the radiofrequency (RF) fields. In the NMR probe circuit, the RF fields are highly attenuated at the ends of the coil and it was experimentally observed that nearly the entire NMR signal comes from the central 2/3 of the sample volume specified by the manufacturer. Hence, in the 6 mm rotor, longer spacers were used to restrict samples to this central 2/3 volume($\sim 160 \, \mu l$). For the 4 mm rotor, the total possible rotor sample volume was $\sim 70 \, \mu l$.

The detection channel was tuned to 13 C at 100.2 or 100.8 MHz, the decoupling channel was tuned to 1 H at 398.6 or 400.8 MHz, and the third channel for REDOR-filtered 1D spectra was tuned to 15 N at 40.4 or 40.6 MHz. 13 C chemical shift referencing was done using the methylene resonance of solid adamantane at 38.5 ppm. 8 The 15 N transmitter was set to ~ 115 ppm using solid (15 NH₄) $_2$ SO₄ as a chemical shift reference at 20 ppm. The 13 C π pulse rf field, 1 H π /2 pulse field, 1 H and 13 C CP fields, and 15 N π pulse field using leucine which contained 5% U- 13 C, 15 N molecules diluted in natural abundance material. The MAS frequency was 8000 \pm 2 Hz for the 1D REDOR experiments and 6800 Hz for the 2D 13 C/ 13 C correlation experiments.

1D REDOR Experimental Details

For the REDOR experiments, generation of ¹³C transverse magnetization was followed by a REDOR dephasing period and then direct ¹³C detection. For the HFP-U3 sample, the ¹³C transmitter was set to 155 ppm at -50 °C and to 100 ppm at 20 °C. ¹³C transverse magnetization was generated using ¹H-¹³C CP with a 53–57 kHz ¹³C ramp and 1.8 ms contact time at -50 °C and 3 ms contact time at 20 °C. The dephasing period was set to 8 rotor periods (1 ms) and contained a single 55 kHz ¹³C refocusing π pulse at the

center of this period. For the S_1 acquisition, 45 kHz ¹⁵N π pulses were applied at the middle and end of every rotor cycle during the dephasing period except for the fourth and eighth cycles. The S_0 acquisition did not contain these ¹⁵N π pulses. In the dephasing period, pulse timing was not actively synchronized to the rotor position. Two-pulse phase modulation (TPPM) ¹H decoupling at 100 kHz was applied during both dephasing and detection with 5.4 μ s pulse length and 90° and 105° phases. ⁹ To obtain optimal compensation of B_0 , B_1 , and MAS frequency drifts, S_0 and S_1 free induction decays (FIDs) were acquired alternately. The recycle delay was 2 s at –50 °C and 1.3 s at 20 °C.

A Z-filter sequence was used to set the 13 C π pulse length and contained the following sequential elements: 1 H- 13 C CP; 13 C π /2; 10 ms; 13 C π ; detection. 1 H decoupling was applied during pulses and detection. The 15 N π pulse length was set by minimization of S₁ signals for the model compound and the TPPM pulse length was set by maximization of the S₀ signal for the model compound.

For each S_1 transient, XY-8 phase cycling was applied to the ¹⁵N π pulses. ^{10,11} Individual S_0 or S_1 transients were coadded with the following phase cycling scheme: ¹H $\pi/2$, x, -x, x, -x; ¹³C CP and ¹³C π , -y, -y, x, x; receiver, x, -x, y, -y. After completion of data acquisition, the sum of S_1 FIDs was subtracted from the sum of S_0 FIDs. Spectral processing was done on the difference FID with a DC offset correction, 25 Hz Gaussian line broadening, Fourier transform, and baseline correction.

2D Experimental Details

The 2D 13 C- 13 C correlation spectra were obtained at -50 $^{\circ}$ C with the probe configured for double resonance 13 C/ 1 H operation. The 13 C sensitivity in double resonance mode was ~ 1.5 times greater than the sensitivity in triple resonance mode. For

one data set, correlations were generated by the proton-driven spin diffusion (PDSD) pulse sequence: $CP - t_1 - \pi/2 - \tau - \pi/2 - t_2$ (figure 7) where t_1 was the evolution period, the first $\pi/2$ pulse rotated ^{13}C transverse magnetization to the longitudinal axis, τ was a 10 ms spin diffusion period during which ^{13}C longitudinal magnetization was transferred between ^{13}C nuclei connected by a network of direct $^{13}C^{-13}C$ bonds, the second $\pi/2$ pulse rotated ^{13}C longitudinal magnetization to the transverse plane, and t_2 was the detection period. Continuous wave (CW) ^{1}H decoupling at 100 kHz was applied during the pulse, t_1 , and t_2 periods, but not during τ . In a second data set, longitudinal transfer of ^{13}C magnetization during τ was achieved with use of the radiofrequency-driven dipolar recoupling (RFDR) method (figure 8). In this approach, a ^{13}C π pulse was applied at the end of rotor cycles 1, 3, 5, ..., 31 during τ . CW ^{1}H decoupling at 100 kHz was also applied during τ . The τ period contained a total of 32 rotor cycles.

The following parameters were common to the PDSD and RFDR data sets: 44-64 kHz ramp on the 13 C CP rf field; 2 ms CP contact time; 50 kHz 13 C $\pi/2$ pulse rf field; 25 μ s t₁ dwell time; 20 μ s t₂ dwell time; and 1 s recycle delay. Hypercomplex data were obtained by acquiring two individual FIDs for each t₁ point with either a 13 C ($\pi/2$)_x or ($\pi/2$)_y pulse at the end of the t₁ evolution period. For the first of these t₁ FIDs, individual transients were coadded with the following phase cycling scheme: first 13 C $\pi/2$ pulse, x, -x, x, -x, x, -x, x, -x; second 13 C $\pi/2$ pulse, x, x, y, y, -x, -x, -y, -y; receiver, y, -y, -x, x, -y, y, x, -x. For the other t₁ FID, the first 13 C $\pi/2$ pulse followed y, -y, y, -y, y, -y, y, cycling. The PDSD data were acquired in ~ 54 hours with 200 t₁ points, 1024 t₂ points, and 1024 transients per FID, and the RFDR data were acquired in ~ 60 hours with 200 t₁ points, 1024 t₂ points, and 512 transients per FID. Both data sets were processed

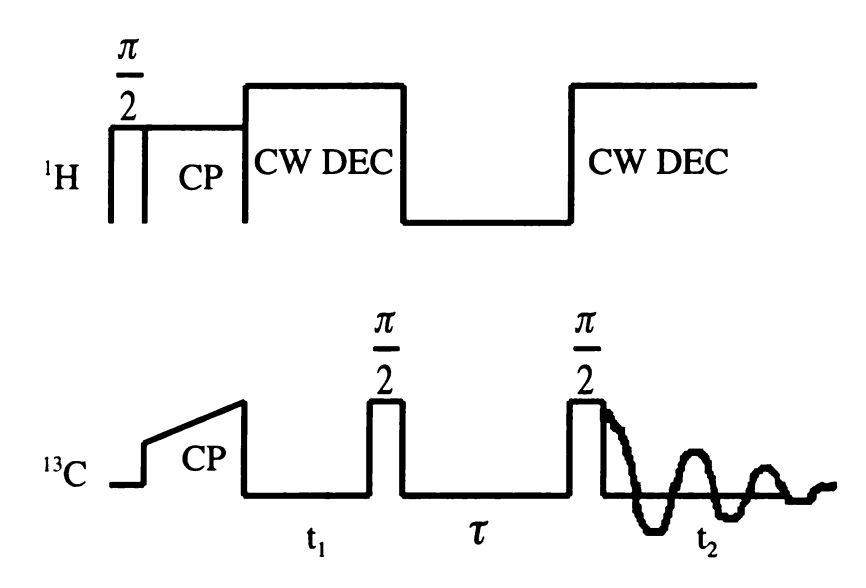


Figure 7. 2D 13 C- 13 C correlation PDSD sequence. Magnetization was transferred from 1 H to 13 C during CP. Continuous wave (CW) decoupling is applied after CP on the protons during t_1 and t_2 , but not during τ . t_1 was the evolution time, τ was the magnetization exchange time, and t_2 was the acquisition time.

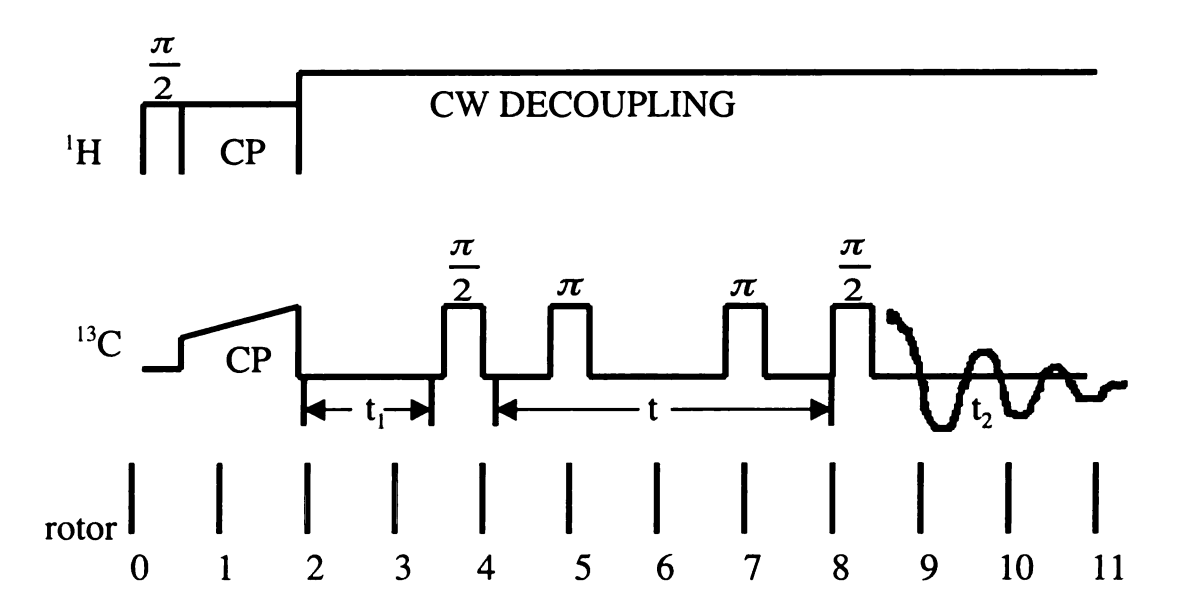


Figure 8. 2D 13 C- 13 C correlation RFDR sequence. CP transferred magnetization from 1 H to 13 C and evolves during t_1 . The τ exchange period consists of 13 C 180° pulses every other rotor period. Acquisition was done during t_2 .

according to the method of States using nmrPipe software. 14,15 Processing included zero-filling, Gaussian line broadening, and baseline correction.

- 1. Chang, C.D., et al., Preparation and Properties of N-Alpha-9-Fluorenylmethyloxycarbonylamino Acids Bearing Tert-Butyl Side- Chain Protection. International Journal of Peptide and Protein Research, 1980. **15**(1): p. 59-66.
- 2. Lapatsanis, L., et al., Synthesis of N-2,2,2-(Trichloroethoxycarbonyl)-L-Amino Acids and N-(9-Fluorenylmethoxycarbonyl)-L-Amino Acids Involving Succinimidoxy Anion As a Leaving Group in Amino-Acid Protection. Synthesis-Stuttgart, 1983. 8: p. 671-673.
- 3. Yang, R., J. Yang, and D.P. Weliky, Synthesis, enhanced fusogenicity, and solid state NMR measurements of cross-linked HIV-1 fusion peptides. Biochemistry, 2003. 42(12): p. 3527-3535.
- 4. Aloia, R.C., H. Tian, and F.C. Jensen, Lipid composition and fluidity of the human immunodeficiency virus envelope and host cell plasma membranes. Proceedings of the National Academy of Sciences of the United States of America, 1993. 90(11): p. 5181-5.
- 5. Hope, M.J., et al., Production of Large Unilamellar Vesicles By a Rapid Extrusion Procedure Characterization of Size Distribution, Trapped Volume and Ability to Maintain a Membrane-Potential. Biochimica Et Biophysica Acta, 1985. 812(1): p. 55-65.
- 6. Yang, J., et al., Application of REDOR Subtraction for Filtered MAS Observation of Labeled Backbone Carbons of Membrane-Bound Fusion Peptides. Journal of Magnetic Resonance, 2002. 159(2): p. 101-110.
- 7. Gullion, T., Introduction to rotational-echo, double-resonance NMR. Concepts in Magnetic Resonance, 1998. 10(5): p. 277-289.
- 8. Morcombe, C.R. and K.W. Zilm, *Chemical shift referencing in MAS solid state NMR*. Journal of Magnetic Resonance, 2003. **162**: p. 479-486.
- 9. Bennett, A.E., et al., *Heteronuclear Decoupling in Rotating Solids*. Journal of Chemical Physics, 1995. **103**(16): p. 6951-6958.
- 10. Gullion, T., D.B. Baker, and M.S. Conradi, New, Compensated Carr-Purcell Sequences. Journal of Magnetic Resonance, 1990. 89(3): p. 479-484.

- 11. Gullion, T. and J. Schaefer, Elimination of Resonance Offset Effects in Rotational-Echo, Double-Resonance NMR. Journal of Magnetic Resonance, 1991. **92**(2): p. 439-442.
- 12. Bennett, A.E., et al., Chemical-Shift Correlation Spectroscopy in Rotating Solids Radio Frequency-Driven Dipolar Recoupling and Longitudinal Exchange.

 Journal of Chemical Physics, 1992. 96(11): p. 8624-8627.
- 13. Bennett, A.E., et al., Homonuclear radio frequency-driven recoupling in rotating solids. Journal of Chemical Physics, 1998. 108(22): p. 9463-9479.
- 14. States, D.J., R.A. Haberkorn, and D.J. Ruben, A Two-Dimensional Nuclear Overhauser Experiment With Pure Absorption Phase in 4 Quadrants. Journal of Magnetic Resonance, 1982. 48(2): p. 286-292.
- 15. Delaglio, F., et al., NMRPipe: a multidimensional spectral processing system based on UNIX pipes [see comments]. Journal of Biomolecular NMR, 1995. 6(3): p. 277-93.

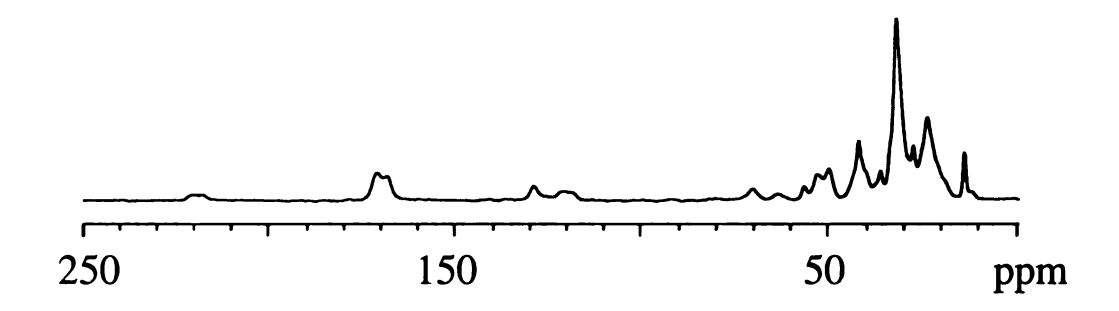
Chapter 3

Results and Discussion - 1D REDOR Filtering and 2D ¹³C-¹³C Correlation

In MAS solid state NMR spectra of membrane-bound peptides and proteins, signals from specifically labeled nuclei can provide important information about the local structure and structural homogeneity.¹⁻⁴ However, for ¹³C, these labeled nuclei signals are usually poorly resolved from large natural abundance signals of lipid and protein. To filter out these natural abundance signals, REDOR difference spectroscopy was investigated. REDOR difference spectroscopy was shown to be an easy method to implement because it only requires only one sample and uses a fairly simple pulse sequence.

Utility of REDOR Filtering

For the NMR sample HFP-U3 associated with the LM3 lipid/cholesterol mixture at peptide:lipid mol ratio ~0.04, Figure 9 displays the REDOR S_o and difference spectra. In the S_o spectrum, there is significant natural abundance signal from the lipid and peptide. The difference spectrum was taken with a 1.6 ms dephasing time and cleanly shows the signals of backbone carbons directly bonded to labeled ^{15}N . The isotropic C_a , carbonyl, and M = +1, -1, and -2 spinning sidebands of the carbonyls are apparent. In the filtered spectrum, the isotropic Phe-8 and Leu-9 carbonyl signals at 172 ppm are unresolved whereas the 40-55 ppm Phe-8, Leu-9, and Gly-10 C_a signals were all resolved. On the basis of the characteristic chemical shifts of residue-types, we can tentatively assign the 42.5 ppm signal to Gly-10 C_a .



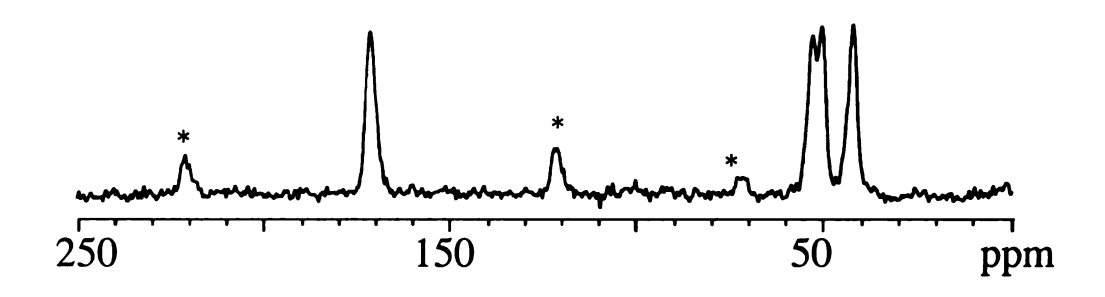


Figure 9. 13 C solid-state NMR spectra of HFP-U3 peptide associated with LM3 lipid mixture at -50° C. (top) Unfiltered REDOR spectrum where signal from both the lipids and peptide are observed. (bottom) Filtered spectrum obtained from the difference of S_{\circ} - S_{1} FIDs. Because of the short 1.6 ms dephasing time only the backbone carbonyl and C_{α} signals from Phe-8, Leu-9, and Gly-10 are observed. * = Carbonyl spinning sidebands

In this case, the difference spectrum is also useful for assessing linewidths and indirectly, the feasibility of doing a full assignment of this peptide with multidimensional NMR methods. The linewidths are a few times larger than those observed in larger U-¹³C, crystalline peptides and proteins, but the recent successes in assignment of these crystalline systems suggest that a fairly long sequence in the membrane-associated fusion peptide can be assigned, followed by a full structure determination. ^{1,6-10}

Comparison of HFP Spectra in Detergent and Membranes

In Figure 10, HFP-U3 was associated with frozen detergent at -80 °C (top) and frozen LM3 membranes at -50 °C (bottom). In both the carbonyl and C_{α} regions of the spectra, there are significant differences in chemical shifts which indicate a change from helical structure in detergent to non-helical structure in LM3. In the C_{α} region, signals are expected from the Phe-8, Leu-9, Gly-10 nuclei, and there are three clear peaks in both the DPC and the LM3 samples. Although site-specific assignment is not definitive in this one-dimensional spectrum, a tentative assignment can be made on the basis of characteristic chemical shifts of particular amino acids. In particular, the C_{α} shifts for Phe, Leu, and Gly in random coil structures are 57.4 ppm, 53.6 ppm, and 43.5 ppm, respectively. When this ordering is used to assign C_{α} peaks in the spectra, the measured shifts for the DPC and LM3 samples lie downfield and upfield of the random coil values, which is consistent with a change for this part of HFP from helical structure in detergent to non-helical structure in LM3. Thus, it appears that there can be significantly different structures in detergent and membranes.

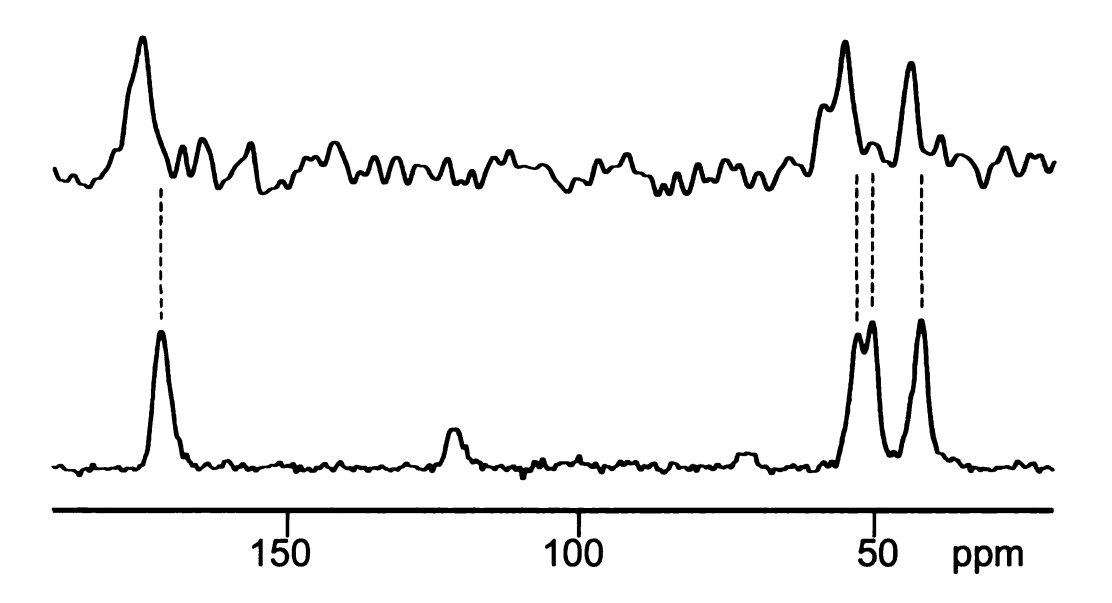


Figure 10. 13 C solid state NMR spectra of HFP-U3 associated with DPC at -80° C (top) and LM3 lipid mixture at -50° C (bottom). The peptide had uniform 13 C , 15 N labeling at the Phe-8, Leu-9, and Gly-10 residues. Because of the 1ms REDOR filter, the spectra are dominated by backbone carbonyl signals from Phe-8 and Leu-9 and backbone C_{α} signals from Phe-8, Leu-9, and Gly-10. For each spectrum, the spinning speed was 8 kHz and 50 Hz gaussian line broadening was applied. The large differences between chemical shifts in (top) and (bottom) spectra are consistent with a change from helical structure in detergent to non-helical structure in LM3.

Temperature Dependence of Spectra

Although physiological fusion occurs at 37 °C, NMR sensitivity is much better at lower temperature and spectra are often obtained at these temperatures. It is therefore important to determine whether lower temperature changes peptide structure. Figure 11 displays the C_a region of the REDOR filtered spectrum of the HIV-1 fusion peptide sample at (top) -50 °C and (bottom) 20 °C. Because of the 1 ms REDOR filter, the displayed spectral regions are dominated by backbone C_{α} signals from Phe-8, Leu-9, and Gly-10. Corresponding peak chemical shifts agree to within 0.5 ppm at the two temperatures, indicating that the lower temperature does not induce a large peptide structural change. The carbonyl region was similarly invariant to temperature. The linewidths were smaller at 20 °C than at -50 °C. For example, for the Gly-10 peak centered at 43.0 ppm, the full-width at half-maximum (FWHM) linewidth is ~ 2.6 ppm at -50 °C and is ~ 1.9 ppm at 20 °C. In addition, the integrated signal-to-noise per ¹³C per transient at 20 °C is approximately 1/3 of its value at -50 °C. For hydrated membrane samples, it is reasonable that motion could increase significantly between -50 °C and 20 °C and this greater motion could explain these experimental observations. For example, increased motion could reduce inhomogeneous broadening and result in smaller linewidths. In addition, motion could attenuate dipolar couplings and decrease the efficiency of ¹H-¹³C cross-polarization (CP) and REDOR dephasing and result in lower REDOR-filtered signal per ¹³C per transient.

2D Correlation Spectra

Figure 12(a) displays a 2D 13 C/ 13 C correlation spectrum for the HFP-U3/LM3 sample and figure 12(b) displays f_2 slices from this spectrum at $f_1 = 137.9$ ppm (upper)

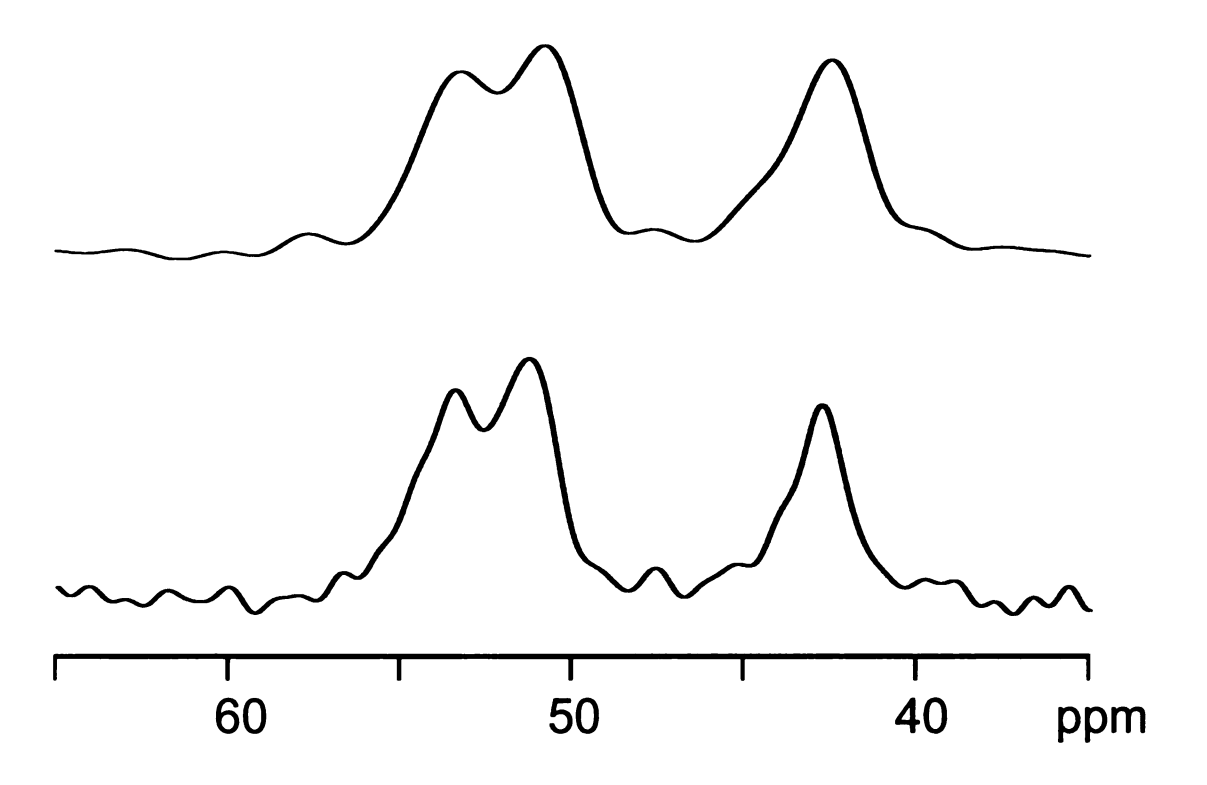


Figure 11. ¹³C solid state NMR spectra of HFP-U3 associated with LM3 lipid mixture at -50 °C (top) and 20 °C. The chemical shifts in the spectra are consistent with non-helical structure at both -50 °C and 20 °C. However, the -50 °C spectrum has about three times more integrated signal per scan than the 20 °C spectrum, which can be explained by greater motion at 20 °C.

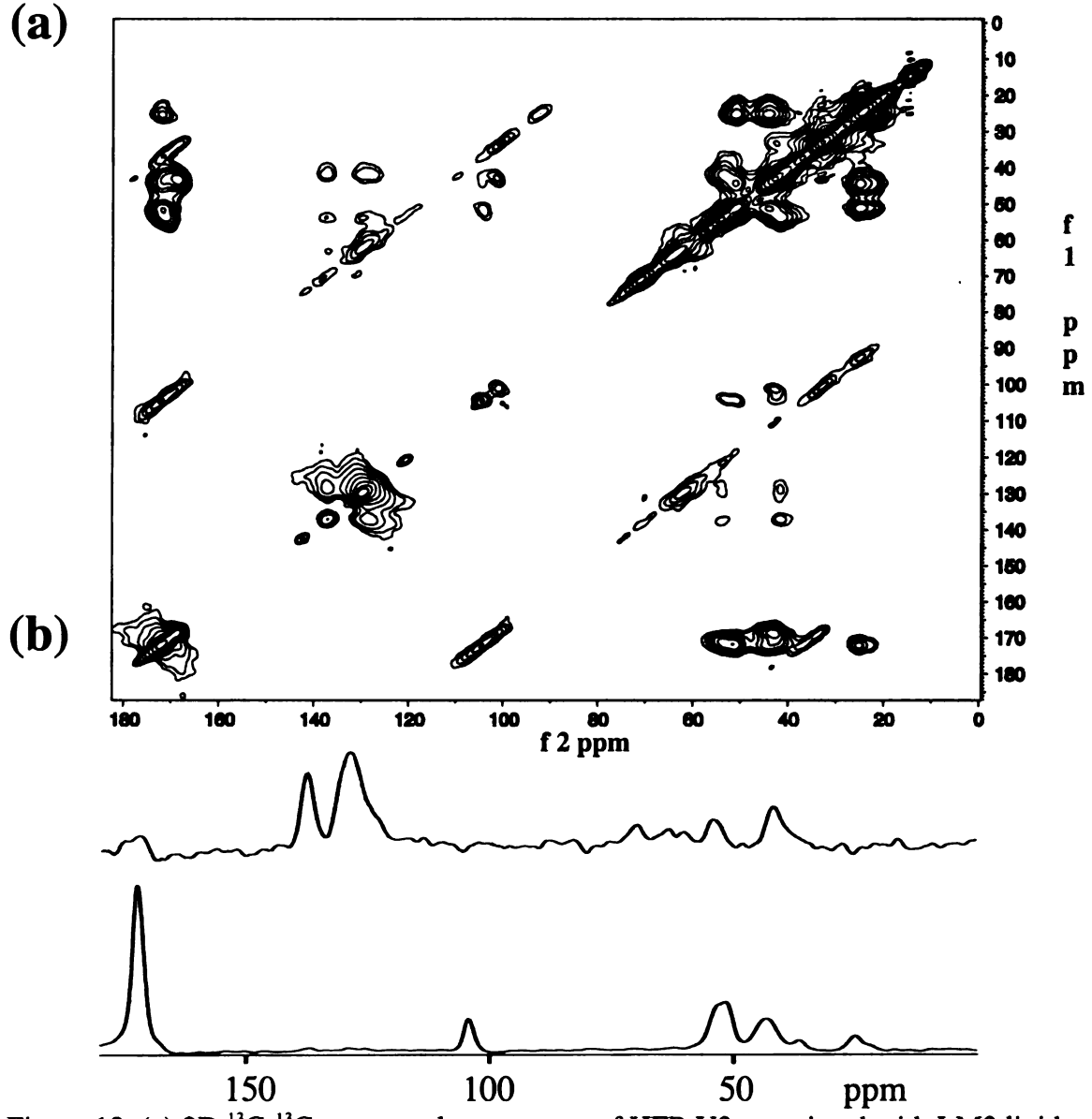


Figure 12. (a) 2D 13 C- 13 C contour plot spectrum of HFP-U3 associated with LM3 lipid mixture at -50 $^{\circ}$ C and (b) f_2 slices from this spectrum. The peptide: lipid mol ratio was \sim 0.04, the buffer pH was 7.0, and the sample volume in the 4mm diameter rotor was \sim 30 μ l. The peptide had uniform 13 C, 15 N labeling at the Phe-8, Leu-9, and Gly-10 residues. The 2D data were obtained with a proton-driven spin diffusion sequence and the total signal averaging time was \sim 54 hours. The spectrum displayed in (a) was processed with 200 Hz Gaussian line broadening in f_1 and 150 Hz line broadening in f_2 . Ten contours are shown with each increasing contour representing 1.5 times greater signal intensity. In the upper slice of (b), cross peaks to the Phe-8 aromatic C1 (f_1 = 137.6 ppm) are displayed. From left to right, they represent magnetization in f_2 on the following Phe-8 nuclei: CO, aromatic C1(diagonal), aromatic C2-C6, C_{α} , and C_{β} . In the lower slice of (b), cross peaks to the Leu-9 CO (f_1 = 172.1ppm) are displayed. From left to right, they represent magnetization in f_2 on the following Leu-9 nuclei: CO (diagonal), CO (m =-1 spinning sideband), C_{α} , C_{β} , C_{γ} with C_{δ} shoulder, and CO (m = -2 spinning sideband).

and 172.1 ppm (lower). The displayed spectra were generated from -50 °C data and the correlations were a result of magnetization exchange driven by 10 ms proton-driven spin diffusion (PDSD). A 2D correlation spectrum with similar appearance (figure 13) was obtained from data for which the magnetization exchange was generated by a 4 ms radiofrequency-driven dipolar recoupling (RFDR) sequence. Measurement of the cross peak chemical shifts and knowledge of 13 C connectivities and characteristic residue-type chemical shifts made possible a full resonance assignment of all of the labeled 13 C in the peptide. For example, the upper slice in fig. 12(b) indicates the f_2 shifts of Phe-8 C_{α} , C_{β} , and CO by means of their correlations with the unique f_1 shift of Phe-8 aromatic C1. The full assignment is presented in Table 1. Each chemical shift entry in Table 1 is the average of 4 and 14 f_1 and f_2 shift measurements from PDSD and RFDR spectra. There was a typical standard deviation of ~ 0.2 ppm in the shift distribution of a single entry.

Figure 14 presents a graphical secondary shift analysis for CO, C_{α} , and C_{β} nuclei in Phe-8, Leu-9, and Gly-10 where the secondary shift is defined as the difference between the measured and random coil shifts. For this analysis, the literature random coil C_{α} and C_{β} shifts¹³ and CO shifts¹⁴ were reduced by 2.1 and 2.0 ppm, respectively, which accounts for the differences between the solid state NMR referencing to neat TMS and the solution NMR referencing to ~5 mM 3-(trimethylsilyl)-propionate (TSP) and DSS, respectively. For the HFP-U3 sample, the negative CO and C_{α} shifts and positive C_{β} shifts correlate with β strand secondary structure over these three residues. C_{β} shifts correlate with β strand secondary structure over these three residues.

In the PDSD and RFDR spectra, (1) only intra-residue cross peaks were definitively observed and (2) relatively strong cross peaks were observed between 13 C separated by several bonds (e.g. Leu-9 CO/ C_{γ}). These observations are consistent with

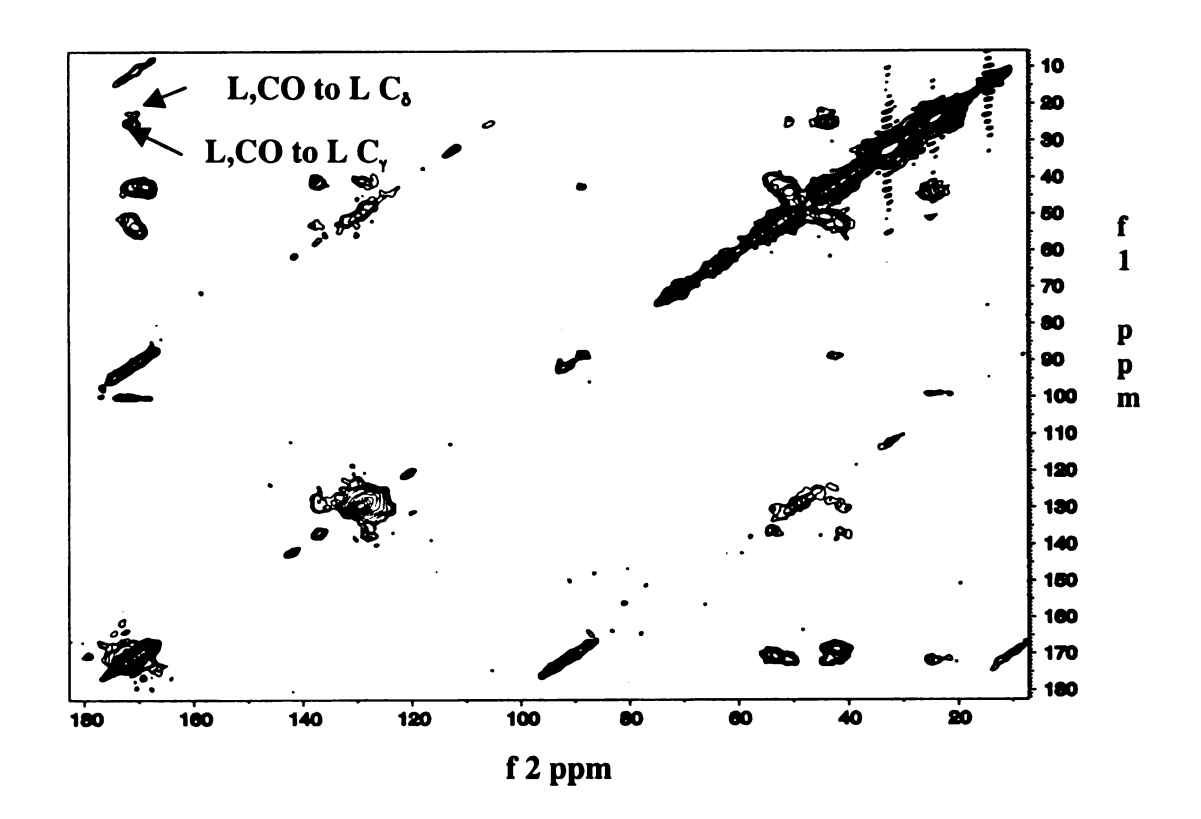


Figure 13. 2D ¹³C-¹³C contour plot spectrum of HFP-U3 associated with LM3 lipid mixture. The 2D data set was obtained with a radio frequency- driven recoupling sequence using a 4 ms RFDR mixing time.

Table 1. ¹³C chemical shift assignments for LM-associated HFP-U3

	C_{α}	C_{β}	C _δ	C _γ	C ar l	C ar 2-6	CO
Phe-8	53.6	41.6			137.3	129.2	171.0
Leu-9	51.2	44.4	25.3	22.5			171.9
Gly-10	42.7						169.1

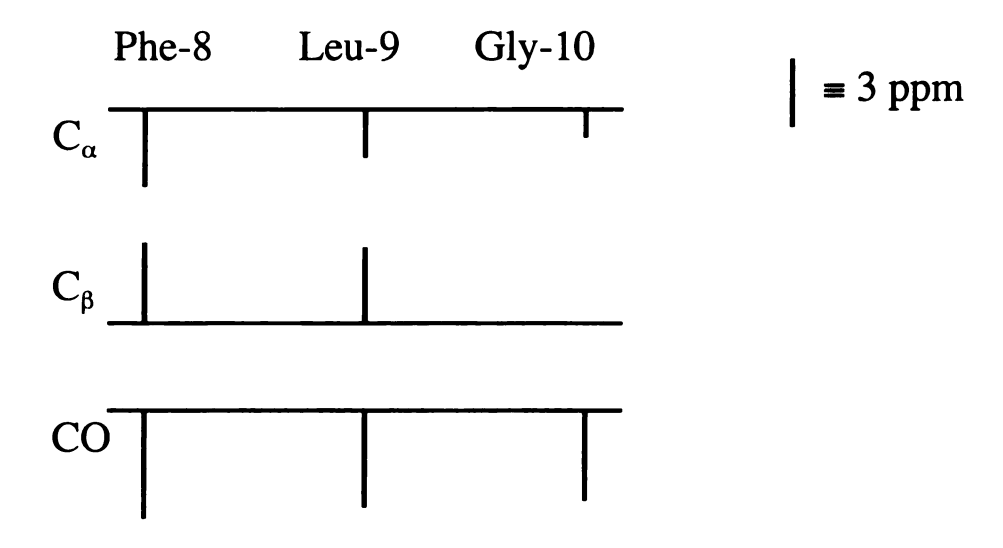


Figure 14. Secondary 13 C chemical shifts for Phe-8, Leu-9, and Gly-10 of HFP-U3 associated with LM3 lipid mixture. Vertical bars represent the secondary shifts for each residue. For these three residues, the pattern shown above is indicative of a β strand structure.

the results of other groups using these experiments with short mixing times on U-13C, 15N labeled peptides and proteins. 7,10,12,19 Both PDSD and RFDR are relatively broad-banded exchange sequences mediated by ¹³C- ¹³C dipolar coupling. For two ¹³C separated by distance r, the exchange rate with have an approximate r⁻⁶ dependence, and direct exchange between ¹³C separated by two bonds or three bonds would respectively occur at ~5% or 2% of the rate of exchange between ¹³C separated by one bond. Thus, it is more likely that a two-bond or three-bond cross peak is due to multiple steps of exchange between directly bonded ¹³C rather than a single step exchange process. With the assumption that there is a single rate constant for directly bonded ¹³C exchange, at short times the ratio of intensities of the two bond/one bond cross peaks will be about the same as the ratio of three bond/two bond cross peaks and the ratio of four bond/three bond cross peaks. This model is qualitatively supported by the relative intensities of the Leu-9 CO/C_{α} , CO/C_{β} , CO/C_{γ} , and CO/C_{δ} , cross peaks (10:6:2:1) and all of the (n+1)/n-bond cross peak intensity ratios are within a range of 0.3 - 0.6. Inter-residue cross peaks are likely not observed in these short mixing time spectra because the ¹⁵N interrupts the direct ¹³C bond network. Inter-residue cross peaks are apparent in a 2D PDSD spectrum with a longer 100 ms mixing time (figure 15), in accord with the experience of other investigators.¹⁰

The success of the complete assignment of the HFP-U3 uniformly labeled peptide associated with LM3 prompted the addition of more uniformly labeled amino acid residues to the sequence. HFP-U12 peptide was synthesized and cross-linked with twelve sequential uniformly ¹³C and ¹⁵N labeled residues between Gly-5 and Gly-16.

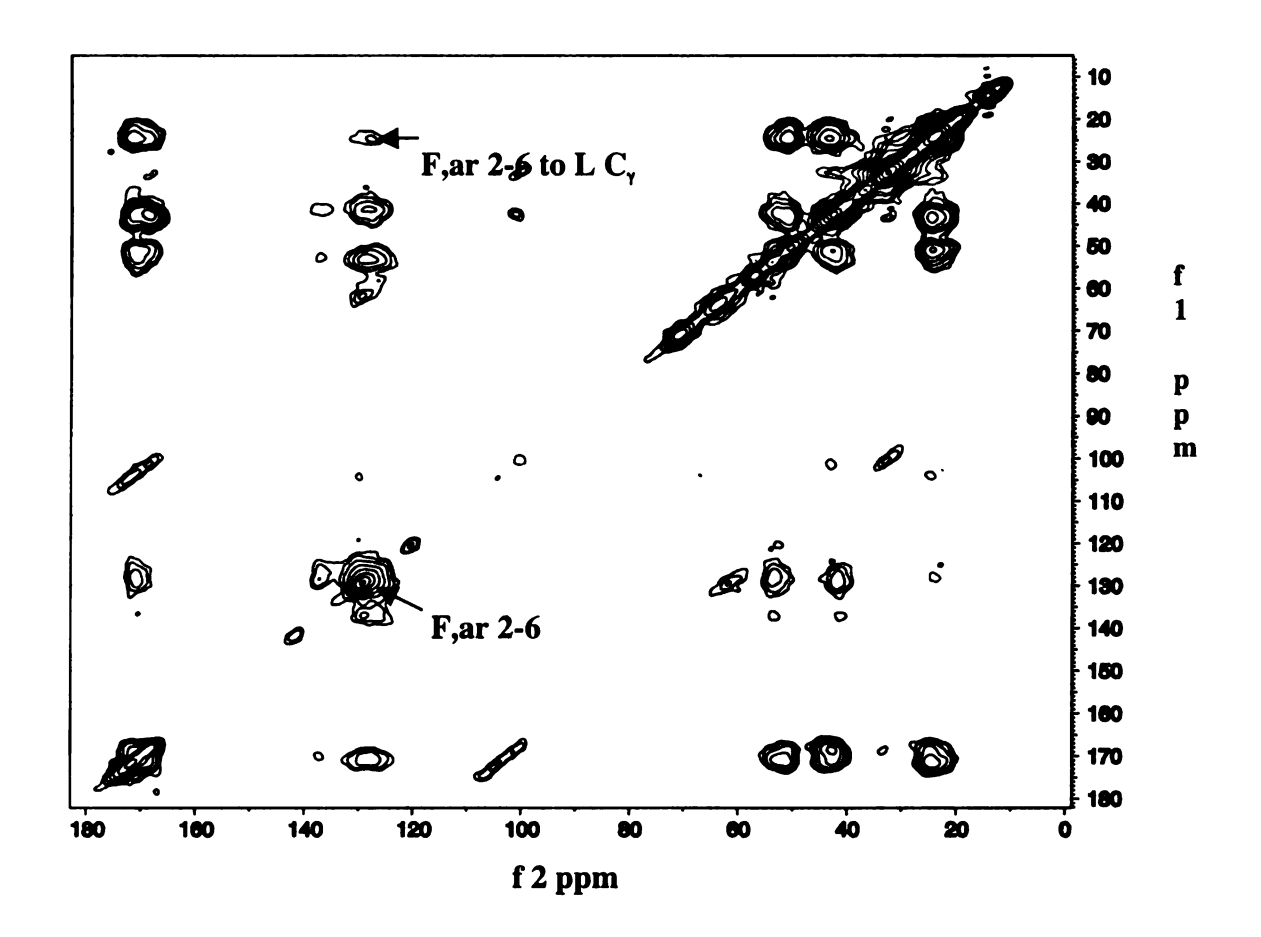


Figure 15. 2D 13 C- 13 C contour plot spectrum of HFP-U3 associated with LM3 lipid mixture at -50 °C. The 2D data was obtained with a proton-driven spin diffusion sequence using a 100ms exchange time. The cross peak between Phe ar. 2-6 and Leu C_{γ} is observed because of the longer exchange time.

Figure 16 displays the REDOR difference spectrum of HFP-U12 associated with LM3 at peptide: lipid mol ratio of ~0.04. The REDOR difference spectrum was taken with a 1 ms dephasing time and shows the signals of backbone carbons directly bonded to labeled 15 N. The isotropic carbonyl signals from the labeled residues at 172.1 ppm and 168.9 ppm are unresolved. This is also true of the C_{α} region of the spectrum where there are three peaks at 42.7 ppm, 49.1 ppm, and 50.8 ppm. Because of the linewidths, it appears from the REDOR difference spectrum that the full assignment of this peptide will be quite challenging even with the use of multidimensional NMR methods.

Figure 17 displays a 2D ¹³C-¹³C correlation spectrum of HFP-U12 dimer associated with LM3. The displayed spectra were obtained from –50 °C data and the observed cross peaks were a result of magnetization exchange driven by 10 ms PDSD exchange time. A 2D correlation spectrum, mediated by RFDR exchange had similar appearance to (figure 18).

In the PDSD and RFDR spectra, intra-residue cross peaks were primarily observed. Because of amino acid degeneracy in HFP-U12, cross peaks could only be assigned as residue-type rather than residue-specific. A residue-type chemical shift assignment of the four different residues is shown in table 2. Higher field may be beneficial for these uniformly labeled systems. In uniformly labeled samples a 40-100 Hz contribution to the ¹³C MAS linewidth is due to unresolved ¹³C-¹³C J-couplings, which in ppm units are inversely proportional to the magnetic field.²⁰ At higher field, linewidths will therefore be narrower and spectral resolution should be improved.

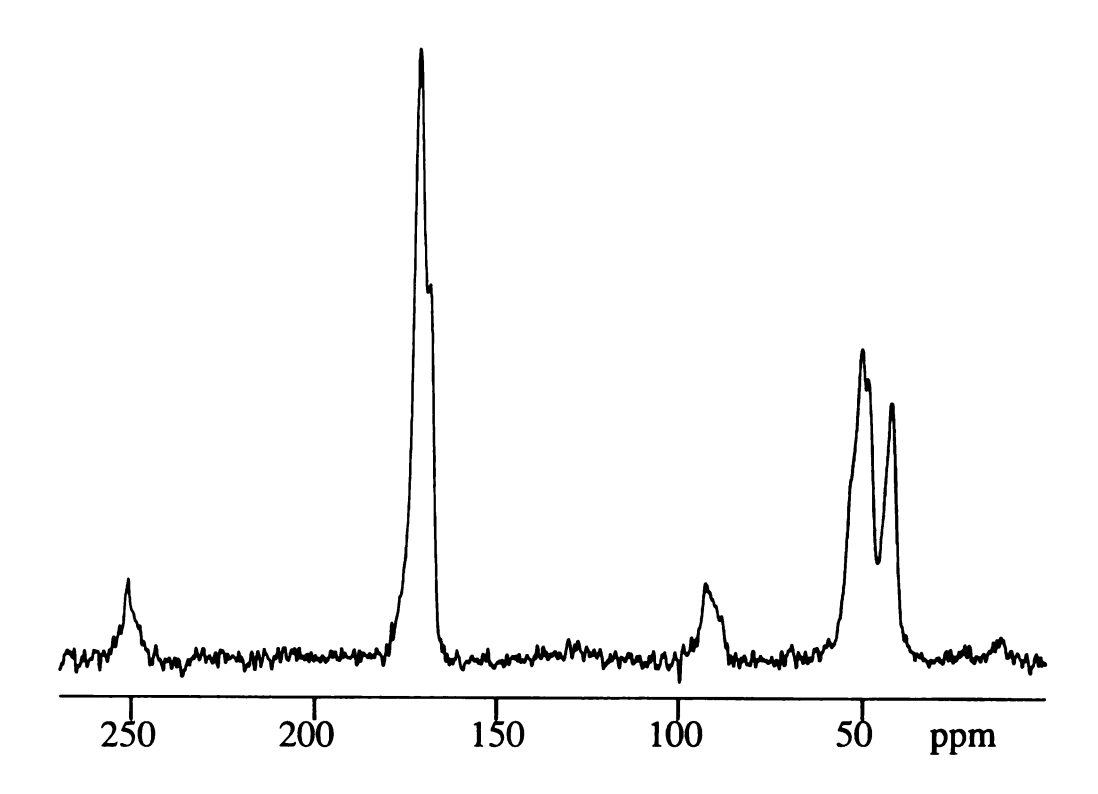


Figure 16. 13 C solid state NMR spectrum of HFP–U12 dimer associated with LM3 at –50°C. Due to a 1 ms REDOR filter time only the backbone carbonyl and C_{α} signals are observed. Other experimental conditions were: 4 mm rotor diameter; 8 kHz MAS frequency; and 50 Hz line broadening.

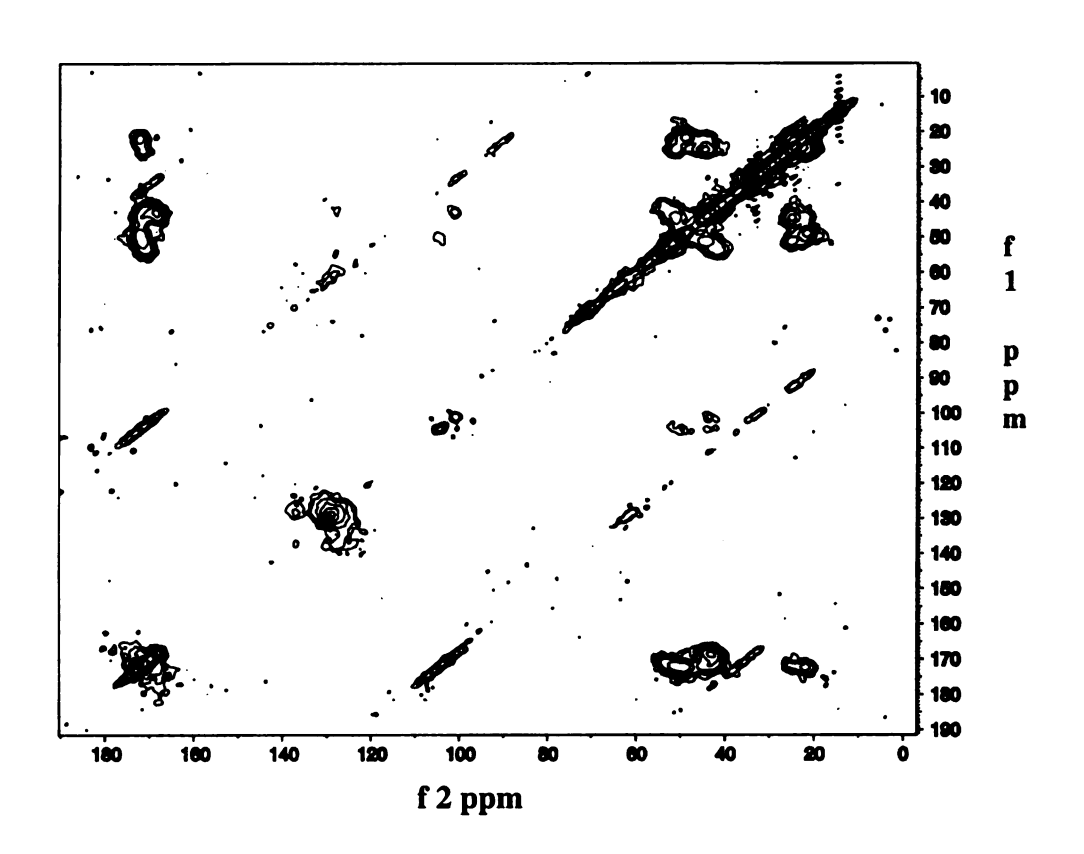


Figure 17. 2D ¹³C-¹³C contour plot spectrum of HFP-U12 dimer associated with LM3 lipid mixture. The 2D data was obtained using a proton-driven spin diffusion sequence with a 10 ms exchange time.

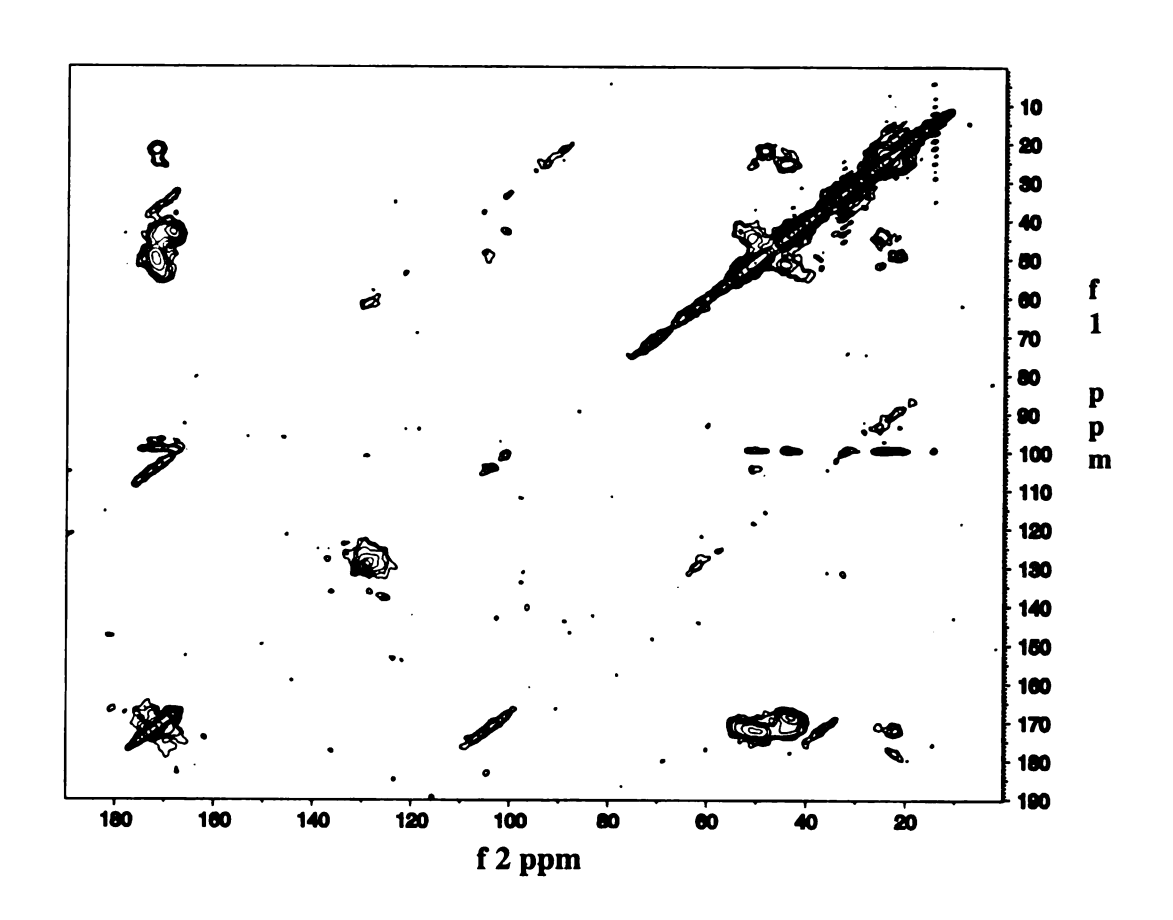


Figure 18. 2D ¹³C-¹³C contour plot spectrum of HFP-U12 dimer associated with LM3 lipid mixture. The 2D data was obtained using a radio frequency-driven recoupling sequence with a 4 ms RFDR mixing time.

Table 2. ¹³C chemical shift assignment for HFP-U12 dimer associated with LM3.

	C_{α}	C_{β}	C_{δ}	C _y	C ar 1	C ar 2-6	CO
Ala	49.1	21.8					172.2
Gly	43.0						168.6
Leu	51.0	44.5	21.8	25.2			171.7
Phe	53.8	42.0			136.7	128.60	171.2

- 1. Smith, S.O., C.S. Smith, and B.J. Bormann, Strong hydrogen bonding interactions involving a buried glutamic acid in the transmembrane sequence of the neu/erbB-2 receptor. Nature Structural Biology, 1996. 3(3): p. 252-8.
- 2. Wang, J., Y.S. Balazs, and L.K. Thompson, Solid-state REDOR NMR distance measurements at the ligand site of a bacterial chemotaxis membrane receptor. Biochemistry, 1997. 36(7): p. 1699-703.
- 3. Yang, J., C.M. Gabrys, and D.P. Weliky, Solid-State Nuclear Magnetic Resonance Evidence for an Extended beta Strand Conformation of the Membrane-Bound HIV-1 Fusion Peptide. Biochemistry, 2001. 40(27): p. 8126-37.
- 4. Yang, J., et al., Solid state NMR measurements of conformation and conformational distributions in the membrane-bound HIV-1 fusion peptide. Journal of Molecular Graphics & Modelling, 2001. 19(1): p. 129-35.
- 5. Evans, J.N.S., Biomolecular NMR Spectroscopy. 1995, New York: Oxford.
- 6. Rienstra, C.M., et al., 2D and 3D N-15-C-13-C-13 NMR chemical shift correlation spectroscopy of solids: Assignment of MAS spectra of peptides. Journal of the American Chemical Society, 2000. 122(44): p. 10979-10990.
- 7. McDermott, A., et al., Partial NMR assignments for uniformly (C-13, N-15)-enriched BPTI in the solid state. Journal of Biomolecular NMR, 2000. 16(3): p. 209-219.
- 8. Detken, A., et al., Methods for sequential resonance assignment in solid, uniformly C-13, N-15 labelled peptides: Quantification and application to antamanide. Journal of Biomolecular NMR, 2001. **20**(3): p. 203-221
- 9. Jaroniec, C.P., et al., Frequency selective heteronuclear dipolar recoupling in rotating solids: Accurate C-13-N-15 distance measurements in uniformly C-13,N-15-labeled peptides. Journal of the American Chemical Society, 2001. 123(15): p. 3507-3519.
- 10. Straus, S.K., T. Bremi, and R.R. Ernst, Side-chain conformation and dynamics in a solid peptide: CP-MAS NMR study of valine rotamers and methyl-group relaxation in fully C-13-labelled antamanide. Journal of Biomolecular NMR, 1997. 10(2): p. 119-128.

- 11. Bennett, A.E., et al., Chemical-Shift Correlation Spectroscopy in Rotating Solids Radio Frequency-Driven Dipolar Recoupling and Longitudinal Exchange.

 Journal of Chemical Physics, 1992. 96(11): p. 8624-8627.
- 12. Bennett, A.E., et al., *Homonuclear radio frequency-driven recoupling in rotating solids*. Journal of Chemical Physics, 1998. **108**(22): p. 9463-9479.
- 13. Spera, S. and A. Bax, Empirical Correlation Between Protein Backbone Conformation and C-Alpha and C-Beta C-13 Nuclear-Magnetic-Resonance Chemical- Shifts. Journal of the American Chemical Society, 1991. 113(14): p. 5490-5492.
- 14. Wishart, D.S., et al., H-1, C-13 and N-15 Random Coil Nmr Chemical-Shifts of the Common Amino-Acids .1. Investigations of Nearest-Neighbor Effects. Journal of Biomolecular NMR, 1995. 5(1): p. 67-81.
- 15. Morcombe, C.R. and K.W. Zilm, *Chemical shift referencing in MAS solid state NMR*. Journal of Magnetic Resonance, 2003. **162**: p. 479-486.
- 16. Wishart, D.S., et al., H-1, C-13 and N-15 Chemical-Shift Referencing in Biomolecular Nmr. Journal of Biomolecular NMR, 1995. 6(2): p. 135-140.
- 17. Saito, H., Conformation-Dependent C-13 Chemical-Shifts a New Means of Conformational Characterization As Obtained By High-Resolution Solid-State C-13 Nmr. Magnetic Resonance in Chemistry, 1986. 24(10): p. 835-852.
- 18. Zhang, H.Y., S. Neal, and D.S. Wishart, *RefDB: A database of uniformly referenced protein chemical shifts*. Journal of Biomolecular NMR, 2003. **25**(3): p. 173-195.
- 19. Pauli, J., et al., Backbone and side-chain C-13 and N-15 signal assignments of the alpha-spectrin SH3 domain by magic angle spinning solid-state NMR at 17.6 tesla. Chembiochem, 2001. 2(4): p. 272-281.
- 20. Marassi, F.M.a.O., S.J, Simultaneous resonance assignment and structure determination in the solid-state NMR spectrum of a membrane protein in lipid bilayers. Biophysical Journal, 2002. 82: p. 2279.

Chapter 4

¹⁵N-¹³C Correlation Experiments

Introduction

In recent years, the problem of structure determination in uniformly labeled 13 C and 15 N biological samples has attracted a considerable amount of interest. Partial and complete assignment of uniformly labeled samples has been done using 2D 15 N/ 13 C and 13 C/ 13 C experiments $^{1-5}$. For sequential assignment, it is particularly interesting to selectively transfer polarization from backbone 15 N to either directly bonded 13 C $_{\alpha}$ or to directly bonded 13 CO and to therefore correlate nuclei within a residue i or between adjacent i and i – 1 residues. Selective 1D 15 N- 13 C transfer experiments can be used to determine the feasibility of implementing these 2D 15 N- 13 C correlation experiments. It is also useful to first optimize the experiments on a high signal-to-noise model compound with completely resolved resonances. Our compound choice for these experiments was crystalline N-Acetyl-leucine.

N-Acetyl-leucine Synthesis and Crystallization

Uniformly ¹³C/¹⁵N labeled leucine was added to acetic acid and heated to 100 °C while stirring. 1-¹³C-acetic anhydride was added, and was stirred until the solid dissolved. The solution was cooled to 80 °C and water was added to react with any excess acetic anhydride. Under reduced pressure the solvent was removed and a viscous liquid remained. Traces of water were removed by the multiple steps of addition of cyclohexane followed by solvent removal under reduced pressure. Solvent removal was considered to be complete when the dry weight no longer changed.⁶ The white solid was

dried further overnight in a vacuum dessicator. Residual acetic acid was then removed by dissolution in water and lyophilization. Solution NMR was used to determine the success of the synthesis.

For crystallization, 16.5 mg of U-N-Acetyl-leucine (figure 19) and 89.4 mg of unlabeled N-Acetyl-leucine were dissolved into ~ 5ml of water under gentle heating. After cooling, the solution was filtered using 0.22 µm sterile syringe filter (Millipore, Bedford) into a clean vial. Crystals were formed upon slow evaporation of the water.

1D ¹⁵N-¹³C Correlation Experiments

The 1D 15 N- 13 C correlation spectra were obtained at -50 $^{\circ}$ C and 6.8 kHz MAS with the pulse sequence: CP1- τ - CP2 – acquisition where CP1 was the 1 H- 15 N cross polarization, τ was 1 μ s, and CP2 was 15 N- 13 C cross polarization (figure 20). The 15 N transmitter was set to 115 ppm and 15 N transverse polarization was generated by 1 H- 15 N CP with a 15 N ramp of 30-49 KHz and a 4.0 ms contact time. 100 KHz CW 1 H decoupling was used during τ , CP2, and acquisition. Polarization was transferred from 15 N to 13 C during CP2 using a 25 KHz field on 15 N with no ramp and 1.5 ms contact time. When the 13 C transmitter was set to 155 ppm, the CP2 transfer was selective for CO and when the 13 C transmitter was set to 60 ppm, the CP2 transfer was selective for C_{α} . The average 13 C CP2 field was 25 KHz for the selective CO transfer and 24.8 KHz for the selective C_{α} transfer.

Results and Discussion

Figure 21 (bottom) displays a ¹³C CP MAS spectrum of the model compound.

The spectrum was taken at -50 °C using 6.8 KHz MAS and processed using 10 Hz

Gaussian line broadening. Two carbonyl peaks are resolved at 177.2 ppm and 175.4 ppm

Figure 19. Chemical structure of U-N-Acetyl-leucine showing ¹³C and ¹⁵N labeling.

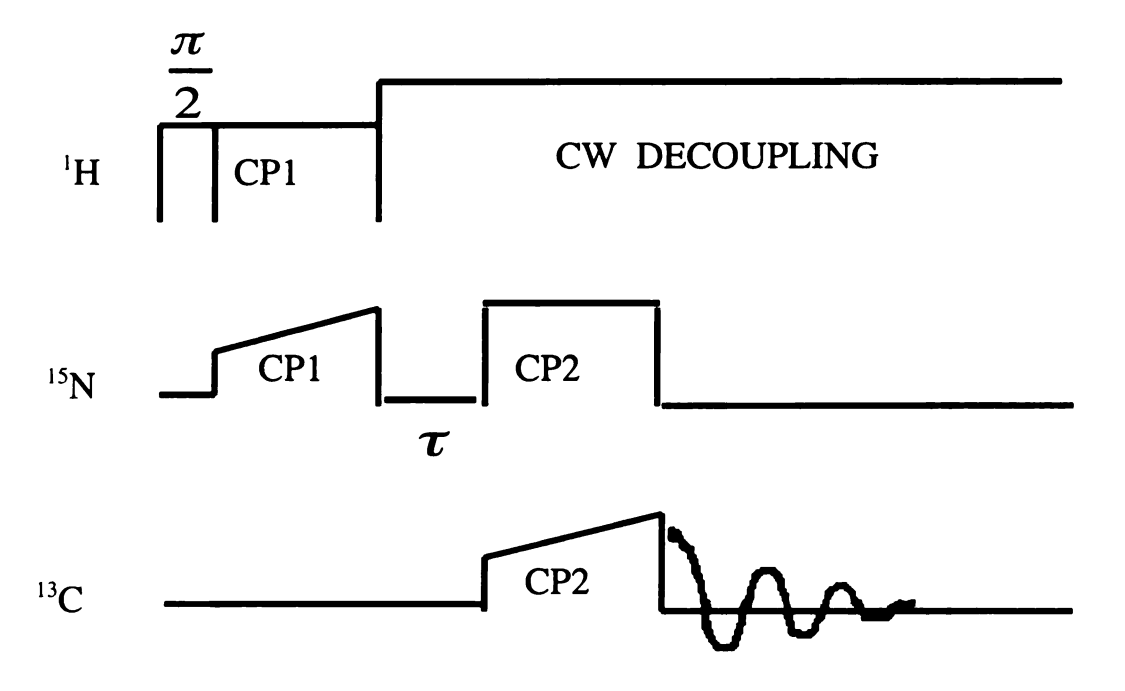


Figure 20. 1D ¹⁵N-¹³C correlation sequence. CP1 transfers magnetization from protons to ¹⁵N. CP2 transfers magnetization from ¹⁵N to ¹³C followed by ¹³C detection.

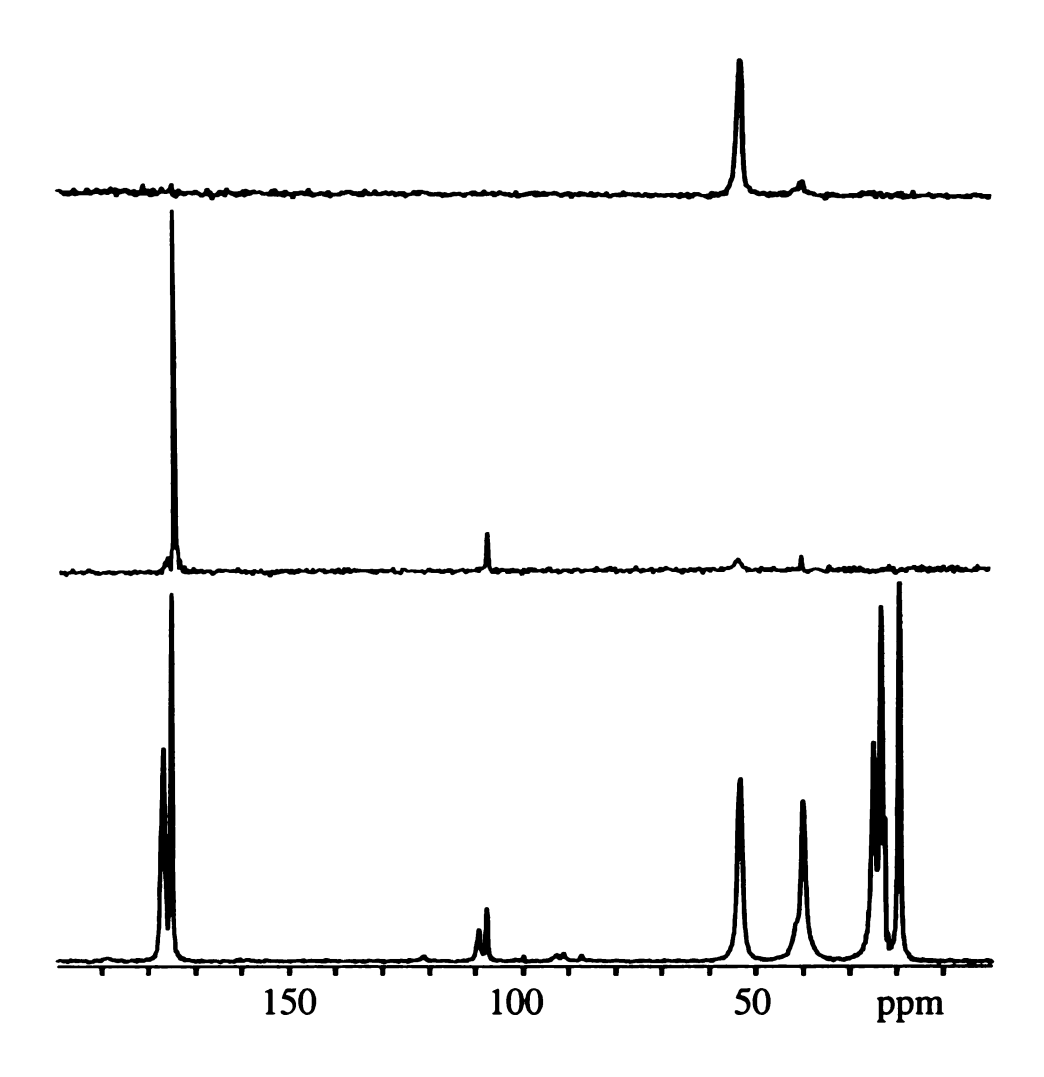


Figure 21. Crystalline N-Acetyl-Leucine model compound uniformly $^{13}\text{C}/^{15}\text{N}$ labeled. The spectra were obtained at -50 °C, MAS frequency of 6.8 kHz ,and 32 scans signal averaging. (bottom) ^{13}C CP MAS all labeled carbons were observed. (middle) 1D $^{1}\text{H-}^{15}\text{N-}^{13}\text{C}$ selective CP spectrum dominant signal from the carbonyl directly bonded to ^{15}N . (Top) 1D $^{1}\text{H-}^{15}\text{N-}^{13}\text{C}$ selective CP spectrum dominant signal from the C_{α} .

where the upfield shift is due to the carbonyl carbon directly bonded to the ^{15}N and the downfield shift is due to the carbonyl bonded to the oxygen. Five peaks are observed in the aliphatic region of the spectrum and had chemical shifts of 53.8, 40.5, 25.5, 23.9, and 20.0 ppm. The signals arose from the C_{α} , C_{β} , C_{γ} , C_{δ} , and the methyl carbon respectively. Integrated intensities from the CO directly bonded to the ^{15}N and the alpha carbon were used to determine the efficiency of the selective 1D ^{15}N - ^{13}C experiments.

Figure 21 (middle) displays a selective $^{15}N^{-13}C$ correlation spectrum. A single peak was observed at 175.4 ppm, which corresponds to the chemical shift of the CO carbon directly bonded to the ^{15}N . For selective CP from ^{15}N to the alpha carbon a single peak at 53.8 ppm was the primary observed (figure 21 top). The chemical shifts of both selective experiments correspond to chemical shifts in the ^{13}C CP MAS experiment. The integrated intensities of CO and C_{α} peaks were measured for both the $^{15}N^{-13}C$ selective CP and ^{13}C CP MAS experiments to determine the efficiencies of the selective CP experiments. Both efficiencies were quite similar with 30% for C_{α} and 33% for CO. The observed efficiencies suggest that it is reasonable to apply these experiments to peptide/lipid samples.

Conclusions

U-N-Acetyl-leucine has been very useful as a model compound to determine the feasibility of the 15 N- 13 C correlation experiments on biologically relevant samples. An efficiency of ~30% for both CO and C_{α} selective experiments was observed and suggests that with sufficient signal averaging time, 15 N- 13 C experiments could be applied to membrane-associated fusion peptide samples.

- 1. Rienstra, C.M., et al., 2D and 3D N-15-C-13-C-13 NMR chemical shift correlation spectroscopy of solids: Assignment of MAS spectra of peptides. Journal of the American Chemical Society, 2000. 122(44): p. 10979-10990.
- 2. McDermott, A., et al., Partial NMR assignments for uniformly (C-13, N-15)-enriched BPTI in the solid state. Journal of Biomolecular NMR, 2000. 16(3): p. 209-219.
- 3. Pauli, J., et al., Backbone and side-chain C-13 and N-15 signal assignments of the alpha-spectrin SH3 domain by magic angle spinning solid-state NMR at 17.6 tesla. Chembiochem, 2001. 2(4): p. 272-281.
- 4. Castellani, F., et al., Structure of a protein determined by solid-state magic-angle-spinning NMR spectroscopy. Nature, 2002. **420**(6911): p. 98-102.
- 5. Detken, A., et al., Methods for sequential resonance assignment in solid, uniformly C-13, N-15 labelled peptides: Quantification and application to antamanide. Journal of Biomolecular NMR, 2001. 20(3): p. 203-221.
- 6. Williamson, K.L., *Macroscale and Microscale Organic Experiments*. second ed. 1994, Lexington, Massachusetts, Toronto: Heath and Company. 632-635.

Chapter 5

Conclusions and Future Work

Temperature Dependence of Spectra

Viral/target cell membrane fusion occurs at 37 °C, but for membrane-associated HIV-1 FP samples, the signal-to-noise per peptide ¹³C per transient is about three times higher at -50 °C. In order to take advantage of the higher signal at low temperatures, it is important to demonstrate the biological relevance of the cold samples and to therefore investigate whether cooling changes the peptide structure. The chemical shifts are similar at 20 °C and at -50 °C, which suggests that cooling does not change the average peptide structure. The temperature dependences of intensities and linewidths do suggest that motion at 20 °C is attenuated at -50 °C, which is a physically reasonable result for hydrated membrane samples.

2D ¹³C-¹³C and ¹⁵N-¹³C Correlation

 13 C/ 13 C correlation spectra of the HFP-U3/LM3 sample were used to give insight into the secondary structure over the three uniformly labeled residues in the peptide chain. Both PDSD and RFDR sequences were used to determine the chemical shift of each labeled carbon nucleus. The difference between the measured and random coil shifts were used to determine the secondary structure. For the HFP-U3/LM3 sample negative CO and C_{α} shifts and positive C_{α} shifts were calculated. This pattern is diagnostic of a β strand secondary structure over the three labeled residues.

We are working on 2D 15 N- 13 C correlation experiments, which will aid in the complete structure determination of the uniformly labeled HIV-1 samples. The correlations are generated by: CP $1-t_1-CP2-t_2$ (figure 22) where CP1 is cross polarization from 1 H- 15 N, t_1 is the evolution period, CP2 is cross-polarization from 15 N- 13 C, and t_2 is the acquisition time. $^{1-5}$ Cross-polarization between 15 N- 13 C can be applied selectively, where magnetization is transferred from the 15 N nuclei to the carbonyl carbon or the alpha carbon. By selectively controlling the transfer of magnetization we can 'walk' down the backbone of the peptide.

2D ¹³C-¹³C correlation spectra of HFP-U12 dimer associated with LM3 showed that only residue type chemical shifts could be obtained at 400 MHz. However, the spectra should be better resolved at higher field (for example 600 or 900 MHz) because of narrower resonances arising from attenuation of ¹³C-¹³C J- and dipolar couplings. In addition, sensitivity should be improved at higher field and will be beneficial for sequential assignment based on 3D experiments such as ¹⁵N-¹³C-¹³C correlation.

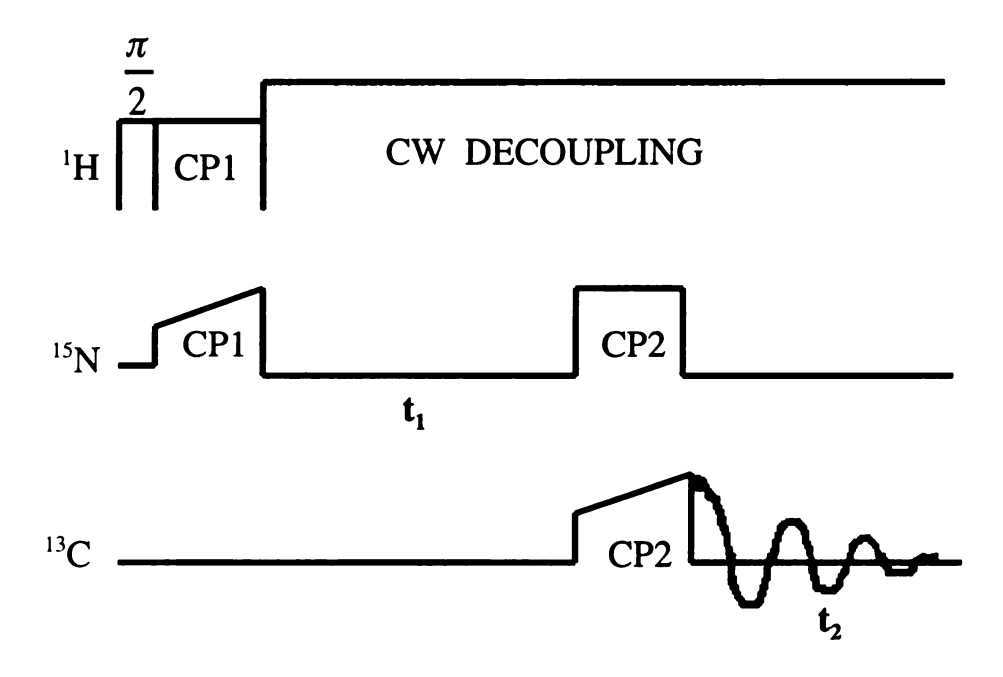


Figure 22. 2D 15 N- 13 C correlation sequence. CP1 transferred magnetization from protons to 15 N, which then evolved during t_1 . CP2 transferred magnetization from 15 N to 13 C and was detected during t_2 .

- 1. Rienstra, C.M., et al., 2D and 3D N-15-C-13-C-13 NMR chemical shift correlation spectroscopy of solids: Assignment of MAS spectra of peptides. Journal of the American Chemical Society, 2000. 122(44): p. 10979-10990.
- 2. McDermott, A., et al., Partial NMR assignments for uniformly (C-13, N-15)-enriched BPTI in the solid state. Journal of Biomolecular Nmr, 2000. 16(3): p. 209-219.
- 3. Pauli, J., et al., Backbone and side-chain C-13 and N-15 signal assignments of the alpha-spectrin SH3 domain by magic angle spinning solid-state NMR at 17.6 tesla. Chembiochem, 2001. 2(4): p. 272-281.
- 4. Egorova-Zachernyuk, T.A., et al., Heteronuclear 2D-correlations in a uniformly [C-13, N-15] labeled membrane-protein complex at ultra-high magnetic fields. Journal of Biomolecular Nmr, 2001. 19(3): p. 243-253.
- 5. Detken, A., et al., Methods for sequential resonance assignment in solid, uniformly C-13, N-15 labelled peptides: Quantification and application to antamanide. Journal of Biomolecular Nmr, 2001. 20(3): p. 203-221.

